UPPSALA
UNIVERSITET

IT Licentiate theses
2014-006

Pulse-modulated Feedback in Mathematical Modeling and Estimation of Endocrine Systems

PER MATTSSON

UPPSALA UNIVERSITY
Department of Information Technology

Pulse-modulated Feedback in Mathematical Modeling and Estimation of Endocrine Systems

Per Mattsson
per.mattsson@it.uu.se

September 2014

Division of System and Control
Department of Information Technology
Uppsala University
Box 337
SE-751 05 Uppsala
Sweden

http://www.it.uu.se/

Dissertation for the degree of Licentiate of Philosophy in Electrical Engineering with Specialization in Automatic Control

ISSN 1404-5117
Printed by the Department of Information Technology, Uppsala University, Sweden

Abstract

This licentiate thesis is concerned with mathematical modeling and estimation of endocrine systems. Hence it also deals with systems biology, a research field that has gained a lot of interest during the last decades. Systems biology can be seen as the systematic study of complex interactions in biological systems, mainly by methods from dynamical systems theory.

The thesis addresses the testosterone (Te) regulation in the human male, but the techniques developed here might be useful for studying other endocrine loops and axes as well.

In the endocrine system of Te regulation, an essential role is also played by the luteinizing hormone (LH) and gonadotropin-releasing hormone (GnRH). Together, these hormones form a closed-loop dynamical system with a pulse-modulated feedback implemented by the pulsatile secretion of GnRH. Mathematical models portraying the interactions between the hormones are instrumental in obtaining insights into the dynamical phenomena arising in the endocrine systems. Such models can also serve as a formal basis for developing strategies of medical interventions.

The contribution of the thesis can be divided into two parts: one covering mathematical models of Te regulation and another suggesting and validating identification techniques for those models.

Regarding mathematical modeling, previously suggested and biologically motivated models of pulsatile Te regulation have been extended to include time delays and nonlinear dynamics, for the purpose of better agreement with clinical data.

In the identification part of the thesis, methods for estimating the unknown parameters in the pulsatile models suggested in the modeling part have been proposed. This part of the thesis also covers model-based estimation of signals that cannot be measured in a non-invasive way. The performance of the developed identification methods is illustrated on simulated and clinical data.

Acknowledgment

I would like to thank my supervisor Professor Alexander Medvedev for his support, guidance, and for sharing his knowledge and expertise throughout this work. A special thank also goes to Professor Alexander Churilov for many interesting and fruitful discussions. And a big thank to all my colleagues at SysCon for providing such a joyful working environment.

I would also like to thank the European Research Council for funding the work done in this thesis under the Advanced Grant 247035 (SysTEAM).

Last but not least I would like to thank my family, without you I would not be the one I am today.

Contents

1 Introduction **7**
1.1 Contribution and publications 7
1.2 Outline of thesis 8

2 The Endocrine System **9**
2.1 Testosterone regulation 9

3 Pulse-modulated feedback **13**
3.1 Pulse-modulated feedback control of linear systems 14
3.2 Time delays 16
3.2.1 Finite-dimensional approximations 16

4 Modeling of endocrine systems **21**
4.1 The Smith Model of Testosterone Regulation 21
4.2 Convolution models 23
4.3 The Pulse-Modulated Smith Model 24
4.3.1 Extensions of the pulse-modulated Smith model . . . 25

Bibliography **27**

Chapter 1

Introduction

The research field of systems biology has gained a lot of interest during the last decades. Systems biology can be seen as the systematic study of complex interactions in biological systems, mainly by methods from dynamical systems theory.

One of the reasons for the success of system biology is that any living organism is a complex system with numerous interacting subsystems, utilizing multiple feedback loops. Thus it fits well into the framework of dynamical systems theory.

There are mainly two different purposes for studying biological systems using mathematical modelling. First it can give new insights into the biological system at hand, and furthermore, these insights together with mathematical tools from e.g. control theory can be used to construct new strategies for medical interventions.

The notions of feedback and feedforward are particularly important in the studies of the endocrine system that uses chemical signaling substances called hormones for communication between cells and organs. The human endocrine system affects all aspects of the physiological and behavioral activities. It is thus of interest to obtain a deeper understanding of the dynamics in the endocrine system, and how failures in this system can be recuperated or circumvented.

1.1 Contribution and publications

This thesis mainly deals with the testosterone (Te) regulation in the human male, but techniques developed here might be useful for studying other parts of the endocrine system too. The contribution of the thesis can be divided into two parts: one covering mathematical models of Te regulation and another suggesting and validating identification techniques for those

models. Regarding modeling, existing models of testosterone regulation have been extended with time delays and nonlinear dynamics, with the purpose of achieving better fit to clinical data. The identification part treats the estimation of unknown model parameters, and estimation of signals that cannot be measured in a non-invasive way.

The thesis comprises the following papers:

Paper I P. Mattsson, and A. Medvedev , *"Estimation of input impulses by means of continuous finite memory observers"*, American Control Conference (ACC), Montréal, Canada, 2012.

Paper II P. Mattsson, and A. Medvedev, *"State Estimation in Linear Time-Invariant Systems With Unknown Impulsive Inputs"*, European Control Conference (ECC), Zürich, Switzerland, 2013.

Paper III A. Churilov, A. Medvedev, and P. Mattsson, *"Periodical Solutions in a Pulse-Modulated Model of Endocrine Regulation With Time-Delay"*, IEEE Transactions on Automatic Control, 59(3): 728–733, 2014.

Paper IV P. Mattsson, and A. Medvedev, *"Modeling of Testosterone Regulation by Pulse-modulated Feedback: An Experimental Data Study"*, International Symposium on Computational Models for Life Sciences, Sydney, Australia, 2013.

Additional material pertaining to the topic of this thesis is presented in the following publications that are not part of this manuscript:

- A. Churilov, A. Medvedev, and P. Mattsson, *"Analysis of a pulse-modulated model of endocrine regulation with time-delay"*, IEEE Conference on Decision and Control (CDC), Maui, USA, 2012.
- A. Churilov, A. Medvedev and P. Mattsson, *"On Finite-dimensional Reducibility of Time-delay Systems under Pulse-modulated Feedback"*, IEEE Conference on Decision and Control (CDC), Florence, Italy, 2013.

1.2 Outline of thesis

This thesis is divided into three major blocks. The first block provides an introduction to endocrine systems in general and testosterone regulation in particular. The second block gives some theoretical background to pulse-modulated systems that are extensively utilized in the appended papers of the thesis. Finally, in the third block, the principles of pulse-modulation are applied to modelling of testosterone regulation in the human male.

Chapter 2

The Endocrine System

The endocrine system consists of all the cells, glands, and tissues that produce hormones inside the body. Hormones are biochemicals that are synthesized by the glands, and secreted into the bloodstream. In this way hormones act as chemical messengers that transfer information between cells, and thus, also organs.

The endocrine system also communicates with the nervous systems through the hypothalamus in the brain. The nervous system sends information to hypothalamus about changes in the body, and regulates the production of hormones in the pituitary gland. In this way both the endocrine and nervous system can use feedback to control physiological and behavioral processes of the organism. Due to feedback loops, the secretion of a hormone is stimulated (or inhibited) by other hormone or hormones. That is, the secretion rate of one hormone depends on the concentration (or concentration change rate) of other hormones. After hormone molecules have been synthesized and released into the bloodstream, they will maintain a biologically active state for a while, and then, like all organic molecules, they will degrade. The process of degradation is referred to as elimination or clearing of hormones.

The above description of the endocrine system, with secretion and elimination rates, as well as feedback loops, indicates that it can be seen as a dynamical system. This thus suggests that the theory of dynamical systems could be useful for modelling and analysis of endocrine systems.

2.1 Testosterone regulation

The endocrine system can be divided into several subsystems that are responsible for different physiological functions. In mammals, one important objective of the endocrine system is to control the reproductive system. In the human male, this is primarily done through the regulation of the male

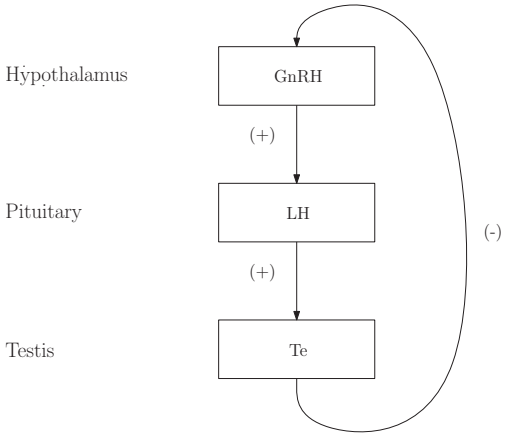

Figure 2.1: Schematic diagram of the male hypothalamic-pituitary-gonadal system. Arrows denote feedforward (stimulatory (+)) and feedback (inhibitory (-)) actions.

sex hormone – testosterone (Te). Testosterone levels are also involved in the growth of muscle, bones and fat tissue, among other things.

The testosterone regulation system is schematically depicted in Fig. 2.1. It mainly comprises two other hormones: luteinizing hormone (LH) and gonadotropin-releasing hormone (GnRH). GnRH is a neurohormone released in the hypothalamus of the brain. GnRH then stimulates the secretion of LH by the pituitary gland. LH travels through the bloodstream to the testes where it stimulates the secretion of Te. Finally, the feedback loop is closed by Te inhibiting the secretion of both LH and GnRH [1]. However, the inhibition of LH has a relatively small effect on the closed-loop system, and is therefore not considered in this thesis.

There are several reasons for studying the dynamics of testosterone regulation in the human male. To start with, a pragmatic reason is that it is one of the simplest endocrine subsystems, involving mainly three different hormones in the axis GnRH-LH-Te. At the same time, the regulation of Te shares many common aspects with regulation in other parts of the endocrine systems, e.g. those handling cortisol, growth hormone, and insulin. Thus, methods developed for modeling of Te regulation in this thesis can hopefully be used for other parts of the endocrine system in the future.

Furthermore, Te regulation, being an integral part of the reproductive system in the human male, constitutes an interesting research topic on its own right. Understanding how the Te regulation works would help planning medical interventions such as testosterone replacement therapy. Accurate

mathematical models can then help researchers to get a deeper insights into the closed-loop dynamics in Te regulation, as well as be an aid in optimizing therapies.

Chapter 3

Pulse-modulated feedback

A typical feedback control system is schematically depicted in Fig. 3. It consists of a dynamical system $\mathcal{S}$, whose output is desired to follow a certain reference signal. This can be achieved by using a feedback controller $\mathcal{C}$ that uses the reference signal and the system output to compute a suitable input signal for $\mathcal{S}$.

The field of control theory started the emerge in the first half of the 20th century [2]. Today, feedback control is an integral part of most engineered systems. A reason for the success of feedback control is that it can create control strategies that perform well even though the components of the system perform poorly, e.g. due to wear and tear. This property is of course also desirable when it comes to the functions inside the human body, so it should come as no surprise that evolution has equipped humans with numerous feedback mechanisms, from the cell level to the level of the complete organism. One such system, equipped with multiple feedback loops of different kinds, is the endocrine system.

In pulse-modulated control, the controller $\mathcal{C}$ feeds the system with a signal that consists of a train of pulses fired at discrete time instants. Due to, among other things, simple realization and low power consumption, this type of control have been used in areas such as electrical, space, heating and pneumatic engineering [3]. Due the pulsatile nature of neural networks and hormone secretion [4], it has also found it uses in modelling of biomedical systems [5].

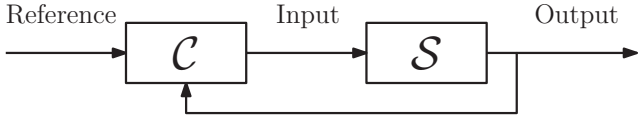

Figure 3.1: Block diagram of a feedback control system

3.1 Pulse-modulated feedback control of linear systems

In pulse-modulated feedback, different pulse types can be used, e.g. rectangular ones. However, here only impulses described by the Dirac delta function $\delta(\cdot)$ are considered. Each impulse in the sequence has a corresponding impulse time t_k and impulse weight λ_k. Arbitrary signal shapes can be created by adding a (known) filter whose impulse response implements the desired pulse shape.

If the plant $\mathcal{S}$ is a linear system with the state vector x and the output y, the pulse-modulated system can be formulated as

$$\dot{x}(t) = Ax(t) + B\xi(t), \quad y(t) = Cx(t), \tag{3.1}$$

where

$$\xi(t) = \sum_{k=0}^{\infty} \lambda_k \delta(t - t_k). \tag{3.2}$$

Note that the impulse at time t_k makes the state vector jump with the amplitude λ_k. Thus system (3.1)-(3.2) can equivalently be formulated as a hybrid system, where the state vector evolves continuously according to a linear equation, but jumps at discrete times t_k:

$$\dot{x}(t) = Ax(t), \qquad \text{if } t \neq t_k \tag{3.3}$$

$$x(t_k^+) = x(t_k^-) + \lambda_k B, \qquad \text{if } t = t_k. \tag{3.4}$$

The time between the impulses, sometimes called the clock interval, will be denoted by $T_k = t_{k+1} - t_k$.

A pulse-modulated system can be controlled in several different ways. In amplitude modulation, the clock intervals T_k are predetermined, e.g. have uniform length, and the amplitude λ_k of each pulse is determined by the control mechanism. In frequency modulation, on the other hand, the length of each clock interval T_k is determined by the controller, while the amplitudes are predetermined.

In this thesis, amplitude-frequency pulse-modulation is used. Here the goal for the controller is to choose both the impulse times t_k and the impulse weights λ_k in such a way that a desired behaviour of the plant is achieved. In the literature, a distinction is typically made between two types of pulse-modulated control. A first possibility is that the length of the clock interval T_k and the corresponding amplitude λ_k are determined directly by the output in the beginning of each interval. That is,

$$t_{k+1} = t_k + T_k, \quad T_k = \Phi(y(t_k^-)), \quad \lambda_k = F(y(t_k^-)), \tag{3.5}$$

for some static functions $\Phi(\cdot)$ and $F(\cdot)$. This type of modulation is refereed to as *modulation of the first kind*.

However, other types of modulation are possible. For example, the next clock interval T_k could be determined as the minimal positive root of the equation

$$T_k = \Phi(\sigma(t_k)), \tag{3.6}$$

where $\sigma(t_k)$ is a function that depends on the output in the interval $[t_{k-1}, t_k]$. In this way, all information from the output can be used to determine the control signal. This is called *modulation of the second kind*.

In the modelling part of this thesis, only modulation of the first kind is considered. One reason for this is that it simplifies the analysis of the dynamical model. Also, only autonomous closed-loop systems are considered, and in this case the behaviour of the controller in between impulse times can in principle be encoded into the modulation functions $\Phi(\cdot)$ and $F(\cdot)$. Hence, concentrating on modulation of the first kind is not a severe restriction in this case.

Assuming that $\Phi(\cdot)$ and $F(\cdot)$ are strictly positive and bounded, the model described by (3.3)-(3.5) is a self-sustained oscillating system. Thus it is of interest to study its periodic solutions. In [6] stability and oscillations of pulse-modulated systems are investigated. Periodical solutions of the specific model given by (3.3)-(3.5) are analyzed in [5] .

From the equations of the model, it is straightforward to derive a map describing how the state vector x propagates from the impulse time t_k to t_{k+1}. That is,

$$x(t_{k+1}^-) = Q(x(t_k^-)), \tag{3.7}$$

where

$$Q(x) = e^{A\Phi(Cx)}(x + F(Cx)B). \tag{3.8}$$

By means of the above equation, different types of periodical solutions of system (3.1),(3.5) can be studied. For example, if x^o is a fixed point of (3.7), i.e.,

$$Q(x^o) = x^o \tag{3.9}$$

then a solution to (3.3)-(3.5) with the initial condition $x(t_0^-) = x^o$ will be periodic with one impulse in each period. Such a solution is called a 1-cycle. In [5], it is shown that a 1-cycle is locally stable if the matrix

$$Q'(x^o) = e^{A\Phi(Cx^o)}[I + F'(Cx^o)BC] + \Phi'(Cx^o)AQ(x^o)C \tag{3.10}$$

is Schur stable, i.e. if the Jacobian $Q'(x^o)$ has all eigenvalues inside the unit circle. There are also similar condition for higher order cycles, see [5]. Bifurcation analysis of the model considered here is carried out in [7], where it is demonstrated that the model can exhibit stable periodic cycles of high multiplicity as well as deterministic chaos.

3.2 Time delays

In many applications, time delays arising between different parts of the studied system play a prominent role. In, for example testosterone regulation, it takes time for LH to travel from the pituitary to the testes. It also takes time for the testes to produce testosterone in response to the LH stimulation.

A time delay can be introduced into the pulse-modulated model in Section 3.1 as

$$\dot{x}(t) = A_0 x(t) + A_1 x(t-\tau) + B\xi(t), \quad y(t) = Cx(t) \tag{3.11}$$

where $\tau \geq 0$. The same type of questions as asked about periodical solutions and stability of the mathematical model in Section 3.1, can also be asked about the time-delay models. Some analytical results regarding (3.11), similar to the ones in [5] for the time delay-free case, are presented in Paper III.

3.2.1 Finite-dimensional approximations

As can be seen in Paper III, the analysis of the system becomes much more involved when time delays are included in the model. For that reason, it might be suitable to see whether a finite-dimensional system can approximately capture the dynamics of (3.11).

When a linear time-invariant system is augmented with a time-delay of length τ, the transfer function will contain the exponential factor $e^{-\tau s}$. A common way to perform finite-dimensional approximation of the time-delay system is to replace $e^{-\tau s}$ with a rational function that approximates the exponential.

Here two approximations of $e^{-\tau s}$ will be considered, namely the Padé approximation [8] and the Laguerre approximation [9]. The Padé approximation is arguably the most common way to approximate a time-delay in a linear system. The Laguerre functions have previously been used to estimate time delays from impulse responses in linear systems [10].

For the time-delayed pulse-modulated system, the transfer function of the linear part (3.11) is given by

$$G(s) = C\left(sI - A_0 - A_1 e^{-\tau s}\right)^{-1} B. \tag{3.12}$$

Replacing $e^{-\tau s}$ with a rational function of order k, gives a rational transfer function $\tilde{G}(s)$ that approximates $G(s)$. Now let $\tilde{A}$, $\tilde{B}$ and $\tilde{C}$ be the system matrices in a state space realization of $\tilde{G}(s)$ and let $x_e(t)$ be the state vector. Then a state-space approximation of (3.12) is

$$\dot{x}_e(t) = \tilde{A}x_e(t) + \tilde{B}\xi(t), \quad \tilde{y}(t) = \tilde{C}x_e(t). \tag{3.13}$$

Note that this model is in the same form as the delay-free case discussed in Section 3.1. Hence, the properties of the approximative system can be studied using the same tools as before. The question is now, does this approximation capture the dynamics of the original model well? There are several ways to answer this. For example, assume that the original system has a stable 1-cycle, will the approximative system have a stable 1-cycle of the same period? Further, will the output $\tilde{y}(t)$ of the approximative system, behave in the same way as the output $y(t)$ of the original system?

Assume the following numerical values in (3.11)

$$A_0 = \begin{bmatrix} -0.4 & 0 & 0 \\ 1 & -0.01 & 0 \\ 0 & 0 & -0.046 \end{bmatrix}, \quad A_1 = \begin{bmatrix} 0 & 0 & 0 \\ 0 & 0 & 0 \\ 0 & 1 & 0 \end{bmatrix}, \tag{3.14}$$

$$B = \begin{bmatrix} 1 \\ 0 \\ 0 \end{bmatrix}, \quad C = \begin{bmatrix} 0 & 0 & 1 \end{bmatrix} \tag{3.15}$$

and choose the modulation functions in (3.5) as

$$\Phi(y) = 50 + 150\frac{(y/r)^2}{1 + (y/r)^2}, \quad F(y) = 1.5 + \frac{5}{1 + (x/r)^2}, \tag{3.16}$$

where $r = 50$ and the time delay is $\tau = 40$. Then (3.11) will have a stable 1-cycle with a period $T_0 = 157.61$. Fig. 3.2 shows how the period $\tilde{T}_0$ of the 1-cycle in the approximative system $\tilde{G}(s)$ behaves for different orders of approximation, both when the Padé and Laguerre functions are used. It can be seen that the Padé approximation converges towards the true period for low orders of approximation. The Laguerre approximation on the other hand does not accurately capture the period well even when the order of approximation is increased to 20.

Fig. 3.3 depicts the output of the original time-delay system in a 1-cycle, as well as the output of the finite-dimensional approximation for different orders of Padé and Laguerre approximations. It can be seen that the Padé approximation has close agreement in signal form already for low approximation orders. For the Laguerre approximation, it can be seen that the signal form gets closer to the true output when the approximation order is increased, but since it does not capture the period of the 1-cycle very well, it will diverge from the true signal after a few periods even for approximation order 20.

These simulations indicate that even though Laguerre functions have been useful in identifying the time-delay in an impulse response, the Padé approximation seems to be preferable when a time delay in a pulse-modulated

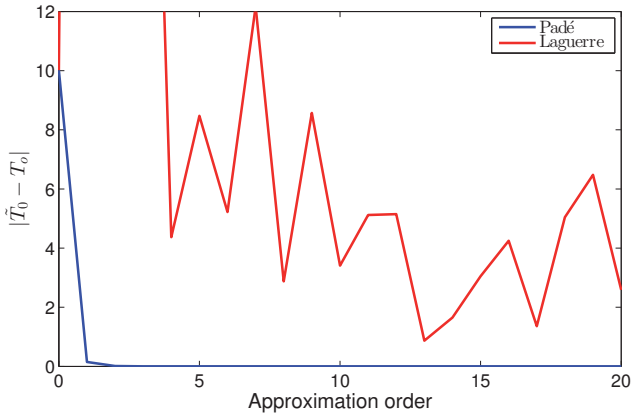

Figure 3.2: The approximation error of a 1-cycles time period for different orders of the Padé and Laguerre approximations. The original infinite dimensional system is given by (3.14)-(3.16), and has a time period $T_0 = 157.61$. The time period $\tilde{T}_0$ of the approximative system varies with the approximation order. The poles of the Laguerre functions are set to 0.15.

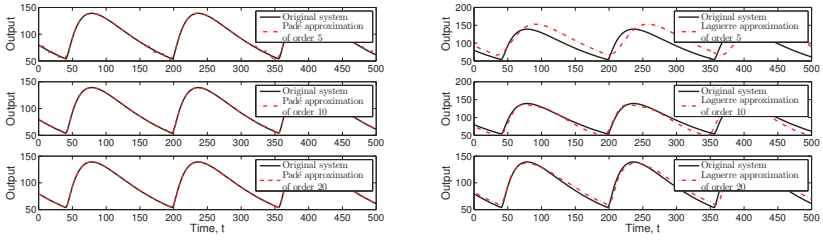

Figure 3.3: Output of the original ($y(t)$) and approximated ($\tilde{y}(t)$) for approximation orders 5, 10 and 20. In the left figure, the Padé approximation is used, and in the right the Laguerre approximation is used.

system is to be approximated. Similar simulations have been carried out with different sets of parameters, with similar results.

The numerical experiments also indicate that already low-order rational approximations of time-delay in systems under pulse-modulated feedback are instrumental in predicting the closed-loop system behaviour. This raises a concern about identifiability of the continuous part of the system from closed-loop data, since it would be difficult to tell whether the dynamics of the system are finite-dimensional or infinite-dimensional. In order to highlight the presence of the time delay, properly injected exogenous excitation could however be used.

Chapter 4

Modeling of endocrine systems

In mathematical modeling of endocrine systems, a number of plausible approaches can be taken. One possibility is to derive a model from the fundamental principles of biology, biochemistry, and physics. This approach has been used in e.g. modeling of the glucose-insulin feedback system in diabetes 1 [11], and in simulating the mechanisms of the human menstrual cycle [12].

However, since endocrine systems usually consist of a complex network of interacting glands and hormones, such models are typically of high dimension and very cumbersome to develop. The complexity of the resulting models also makes it hard to estimate the parameters of the model, as well as using it to develop therapy strategies.

In order to obtain insights into the principles of biological feedback via mathematical analysis, a modeling approach where only the most essential characteristics and interactions of the system are included appears to be useful. Techniques from system identification [13] can then be used to estimate the parameters of the model in a systematic way, yielding a relatively simple model that yet can accurately describe how the hormone concentrations vary with time. This is the approach taken here.

4.1 The Smith Model of Testosterone Regulation

As described in Section 2.1, the endocrine system of Te regulation in the male essentially consists of three hormones, namely Te, LH, and GnRH. GnRH is secreted in an episodic and pulsatile manner in the hypothalamus and stimulates the secretion of LH into the blood by the pituitary gland. LH stimulates, in its turn, the secretion of Te in the testes, see Fig. 2.1.

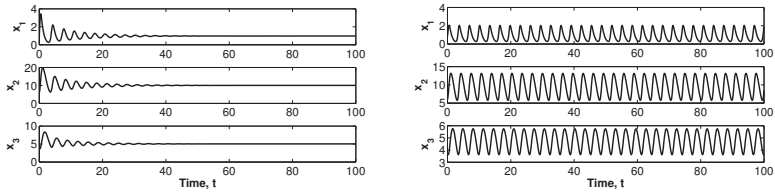

Figure 4.1: Solutions to the Smith model with the nonlinear function f as a Hill function. Left, Hill order $\rho = 7$. Right, Hill order $\rho = 10$.

For example, in [14], a reductionist approach was taken to develop a qualitative mathematical model describing the male reproductive system. The model, usually called the Smith model, can be expressed by the following three ordinary differential equations

$$\begin{aligned} \dot{R} &= f(T) - B_1(R), \\ \dot{L} &= G_1(R) - B_2(L), \\ \dot{T} &= G_2(L) - B_3(T), \end{aligned} \tag{4.1}$$

where $R(t)$, $L(t)$ and $T(t)$ represent the serum concentration of GnRH, LH, and Te, respectively. The non-negative functions B_1, B_2, B_3 describe the clearing rates of the hormones and G_1, G_2, f specify the rates of their secretion. Instead of portraying all the complex interactions between the constituting parts of the endocrine system, the Smith model captures only the main features to match the mathematical tools available at that time.

Since it is well known that the concentrations of LH and Te do not stay at constant levels, only self-sustained oscillating solutions are biologically feasible behaviors of the autonomous model in (4.1). The dynamical properties of (4.1) have been studied analytically to great extent for different choices of the functions B_i, G_i and f. It is relatively common to approximate B_i and G_i by linear functions, so that

$$\begin{aligned} B_i(x) &= b_i x, \quad b_i > 0, i = 1, 2, 3; \\ G_i(x) &= g_i x, \quad g_i > 0, i = 1, 2. \end{aligned} \tag{4.2}$$

In [14], sufficient conditions for (4.1)-(4.2) to have stable periodic solutions are given.

Fig. 4.1 shows two solutions of (4.1)-(4.2) with $f(x)$ chosen to be a Hill function,

$$f(x) = \frac{K}{1 + \beta x^p}. \tag{4.3}$$

It can be seen that the solution converges to a stable stationary point when

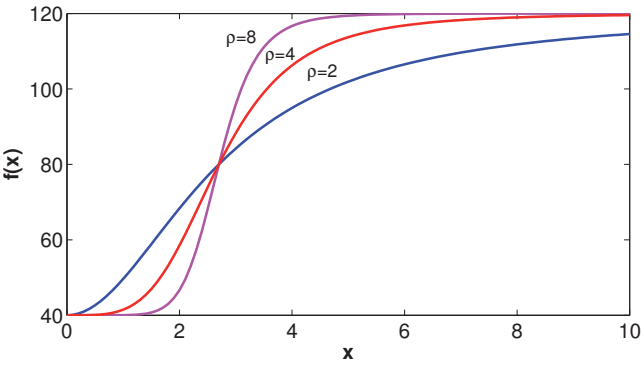

Figure 4.2: The Hill function (4.3) for different values of ρ.

$\rho = 7$, and that the solution is periodic when $\rho = 10$ for the chosen parameter values. In fact, it was shown in [15] that a necessary condition for a periodic solution is that $\rho > 8$, for any choices of the linear parameters. In e.g. [16] and [17], it is argued that such a high value of the Hill function order is unrealistic. Indeed, already for $\rho \geq 4$ (cf. Fig. 4.1), the Hill function in (4.3) resembles a relay characteristic that lacks a proper biological justification.

To resolve the above issue, several attempts have been made to extend the Smith model in such a way that the solutions oscillate for a broader range of the parameters, mostly by introducing special types of nonlinear feedback and time delays. Yet, the Smith model of testosterone regulation in the formulation of [16] is proven to be asymptotically stable for any value of the time delay under a nonlinear feedback in the form of a first-order Hill function, [18]. However, by introducing a non-smooth feedback such as piece-wise linear (affine) nonlinearities, multiple periodical orbits and chaos arise in the Smith model [19, 20]. Multiple delays in the Smith model under a second-order Hill function feedback are also shown to lead to sustained nonlinear oscillations in some subspaces of the model parameters [21].

4.2 Convolution models

As described in Section 4.1, there are several problems with using the classical (continuous) closed-loop Smith model. For this reason, at present, analysis of hormone dynamics from measured (blood serum) hormone concentrations usually only considers open-loop dynamics. It is usually assumed that the concentration of a single hormone satisfies a linear ordinary differential equation of the form

$$\frac{dC(t)}{dt} = -bC(t) + S(t), \tag{4.4}$$

where $C(t)$ is the time profile of the concentration, $S(t)$ the hormone secretion rate, and b is the rate of elimination, see, e.g. [22]. So, if the hormone in question is LH, then $C(t)$ and $S(t)$ correspond respectively to $L(t)$ and $G_1(R(t))$ in the Smith model, while b corresponds to b_2.

For (4.4) it holds that

$$C(t) = \int_0^t S(\tau)E(t-\tau)d\tau + C(0)E(t) \tag{4.5}$$

where $E(t)$ is the impulse response of (4.4), and describes the elimination rate profile of the hormone. A reasonable and often used model for a hormone concentration is therefore the convolution given by (4.5). In order to understand the properties of the endocrine system better, it is of interest to know the time profile of the secretion rate $S(t)$, while only the concentration $C(t)$ is measurable. In this case, deconvolution methods can be used to estimate $S(t)$ from $C(t)$ by exploiting (4.4).

However, if there is no *a priori* information about the secretion profile $S(t)$ or the impulse response $E(t)$, this problem is usually ill-conditioned. Hence, in most cases, some assumptions on the secretion profile are made, resulting in so-called model-based deconvolution. Many algorithms for estimation of hormone secretion rates from concentration data exist, e.g. WEN Deconvolution [23], WINSTODEC [24], and AutoDecon [25]. In [23], a comparison of several different deconvolution approaches is presented.

Most deconvolution-based methods capture major pulsatile secretion events when used on longer time series. However, they tend to neglect the existence of smaller pulses in between major pulses [26]. In [26] some methods for circumventing this problem are proposed. Further, the deconvolution-based methods do not take into account the fact the hormones in the endocrine system are part of a closed-loop system. In order to capture the closed-loop dynamics model-based observers can be utilized, see e.g. [27].

4.3 The Pulse-Modulated Smith Model

It is well known that GnRH is released episodically by hypothalamic neurons in modulated secretory bursts [28]. In e.g. [29], a detailed mathematical description of GnRH pulses is presented.

The pulsatile nature of GnRH is not directly reflected by the classical Smith model in (4.1), where the resulting oscillating temporal profile of the involved hormones is due to smooth nonlinearities.

However, for the purpose of capturing the biologically implemented feedback mechanism, an element implementing pulse-amplitude and pulse-frequency

modulation can be used, as explained in [4]. Thus the mathematical framework of pulse-modulated feedback, discussed in Section 3.1, is directly applicable.

An extended version of the Smith model, that makes use of pulse-modulation was introduced in [5].

In order to extend the Smith model with pulse-modulation, let t_k, $k = 0, 1, 2, \ldots$ be the time instances when a GnRH pulse is released in the bloodstream, and let λ_k represent the size of the pulse number k. Then a pulse-modulated model of testosterone regulation can be written in a state-space form with $x \in \mathbb{R}^3$, and $x_1 = R(t)$, $x_2(t) = L(t)$, $x_3(t) = T(t)$, as

$$\dot{x}(t) = \begin{bmatrix} -b_1 & 0 & 0 \\ g_1 & -b_2 & 0 \\ 0 & g_2 & -b_3 \end{bmatrix} x(t), \qquad \text{if } t \neq t_k \tag{4.6}$$

$$x(t_k^+) = x(t_k^-) + \lambda_k \begin{bmatrix} 1 \\ 0 \\ 0 \end{bmatrix}, \qquad \text{if } t = t_k \tag{4.7}$$

where b_1, b_2, b_3, g_1 and g_2 are the positive parameters as in (4.2). The firing times t_k and the impulse weights λ_k are then given by the recursion

$$t_{k+1} = t_k + \tau_k, \quad \tau_k = \Phi(x_3(t)), \quad \lambda_k = F(x_3(t)), \tag{4.8}$$

where $\Phi(\cdot)$ is a frequency modulation characteristic and $F(\cdot)$ is an amplitude modulation characteristic.

The model in (4.6)-(4.8) is referred to as the pulse-modulated Smith model, and was analyzed in detail in [5]. It constitutes a hybrid system that evolves in continuous time according to (4.6), but undergoes instantaneous jumps in the continuous state vector at discrete points governed by (4.7). Each jump in the state vector corresponds to the secretion of a GnRH impulse.

By construction, this model will, just as the biological system, always have sustained oscillations. It thus solves the problem with stationary solutions in the classical Smith model discussed in Section 4.1. The dynamics of (4.6)-(4.8) are thoroughly studied and are known to exhibit oscillating solutions that are either periodic or chaotic [7].

4.3.1 Extensions of the pulse-modulated Smith model

One of the contributions in this thesis is extensions of the model presented in Section 4.3. The motivation for these extensions is that the model in (4.6)-(4.8) does not reflect some biological properties of the system that manifest themselves in clinical data.

An important property of testosterone regulation, that is not included in the pulse-modulated feedback model, is that it takes time for LH secreted in the pituitary to travel, through the bloodstream, to the testes where Te is produced. In [30], it is suggested that it takes about 5 minutes for LH to travel from the pituitary to the testes. Furthermore, there is a time delay of about 25 minutes between LH stimulation of the testes and the release of Te. Hence it follows that there is a time delay of about 30 minutes from the secretion of LH to the secretion of Te, which is not accounted for in (4.6)-(4.8). In order to add such a time delay, methods described in Section 3.2 are used in Paper III.

Furthermore, because of the linear approximation in (4.2), nonlinear effects are not considered in the pulse-modulated model presented here. Unfortunately, clinical data indicate that saturation actually plays an important role when it comes to LH stimulation of Te secretion. The biological reason for such a saturation is that there is a limited amount of Te that can be produced during any finite time interval, and clinical data demonstrate that the Te secretion rate actually does saturate in some subjects. In Paper IV, a saturating nonlinearity is added to the model, and estimations of the involved parameters are carried out.

Bibliography

[1] J. D. Veldhuis, "Recent insights into neuroendocrine mechanisms of aging of the human male hypothalamic-pituitary-gonadal axis," *Journal of Andrology*, vol. 20, no. 1, pp. 1–18, 1999.

[2] K. J. Åström and P. Kumar, "Control: a perspective," *Automatica*, 2013.

[3] A. K. Gelig and A. N. Churilov, "Frequency methods in the theory of pulse-modulated control systems," *Automation and Remote Control*, vol. 67, no. 11, pp. 1752–1767, 2006.

[4] J. Walker, J. Terry, K. Tsaneva-Atanasova, S. Armstrong, C. McArdle, and S. Lightman, "Encoding and decoding mechanisms of pulsatile hormone secretion," *Journal of Neuroendocrinology*, vol. 22, pp. 1226–1238, 2009.

[5] A. Churilov, A. Medvedev, and A. Shepeljavyi, "Mathematical model of non-basal testosterone regulation in the male by pulse modulated feedback," *Automatica*, vol. 45, no. 1, pp. 78–85, 2009.

[6] A. K. Gelig and A. N. Churilov, *Stability and Oscillations of Nonlinear Pulse-Modulated Systems*. Boston: Birkhäuser, 1998.

[7] Z. T. Zhusubaliyev, A. N. Churilov, and A. Medvedev, "Bifurcation phenomena in an impulsive model of non-basal testosterone regulation," *Chaos: An Interdisciplinary Journal of Nonlinear Science*, vol. 22, no. 1, 2012.

[8] J. Lam, "Convergence of a class of Padé approximations for delay systems," *International Journal of Control*, vol. 52, no. 4, pp. 989–1008, 1990.

[9] P. Mäkilä, "Laguerre series approximation of infinite dimensional systems," *Automatica*, vol. 26, no. 6, pp. 985 – 995, 1990.

[10] E. Hidayat and A. Medvedev, "Laguerre domain identification of continuous linear time-delay systems from impulse response data," *Automatica*, vol. 48, no. 11, pp. 2902 – 2907, 2012.

[11] B. P. Kovatchev, M. Breton, C. Dalla Man, and C. Cobelli, "In silico preclinical trials: A proof of concept in closed-loop control of type 1 diabetes," *Journal of Diabetes Science and Technology*, vol. 3, no. 1, pp. 44–55, January 2009.

[12] N. Rasgon, L. Pumphrey, P. Prolo, S. Elman, A. Negrao, J. Licinio, and A. Garfinkel, "Emergent oscillations in mathematical model of the human menstrual cycle," *CNS Spectrums*, vol. 8, no. 11, pp. 805–814, 2003.

[13] T. Söderström and P. Stoica, *System Identification.* Upper Saddle River, NJ, USA: Prentice-Hall, Inc., 1988.

[14] W. R. Smith, "Hypothalamic regulation of pituitary secretion of luteinizing hormone. II. feedback control of gonadotropin secretion," *Bulletin of Mathematical Biology*, vol. 42, no. 1, pp. 57 – 78, 1980.

[15] L. S. Farhy, "Modeling of oscillations in endocrine networks with feedback," in *Numerical Computer Methods, Part E*, ser. Methods in Enzymology, M. L. Johnson and L. Brand, Eds. Academic Press, 2004, vol. 384, pp. 54–81.

[16] J.D. Murray, *Mathematical Biology, I: An Introduction (3rd ed.).* New York: Springer, 2002.

[17] W. J. Heuett and H. Qian, "A stochastic model of oscillatory blood testosterone levels," *Bulletin of Mathematical Biology*, vol. 68, no. 6, pp. 1383–1399, 2006.

[18] G. Enciso and E. Sontag, "On the stability of a model of testosterone dynamics," *J. Math. Biol.*, vol. 49, pp. 627–634, 2004.

[19] R. Abraham, H. Kocak, and W. Smith, "Chaos and intermittency in an endocrine system model," in *Chaos, Fractals, and Dynamics*, P. Fischer and W. R. Smith, Eds. Marcel Dekker, Inc., 1985, vol. 98, pp. 33 – 70.

[20] C. Sparrow, "Chaos in a three-dimensional single loop feedback system with a piecewise linear feedback function," *J. Math. Anal. Appl.*, vol. 83, no. 1, pp. 275–291, 1981.

Paper I

Estimation of Input Impulses by Means of Continuous Finite Memory Observers

Per Mattsson and Alexander Medvedev*†

Abstract

This paper deals with the estimation of impulsive input signals in systems with linear time-invariant dynamics. The problem arises e.g. in the context of hybrid systems with intrinsic pulse-modulated feedback that have been recently used for mathematical modeling of endocrine systems with pulsatile hormone secretion. In such systems, the impulsive signal generated by a pulse-modulated feedback controller is typically not accessible for measurement. Classical deconvolution-based methods are not directly applicable since the signal to be estimated is unbounded. Instead, a solution making use of continuous finite-memory observers is suggested where both the input impulse weight and its firing time are estimated from the difference of the observers' state estimates. The feasibility of the approach is illustrated by a simulation example.

1 Introduction

Dynamical systems with impulsive control signals appear often in mechanics, power electronics, chemistry and biology, see e.g. [1]. In engineered systems, the controller and, subsequently, the generated control signal are typically known. Therefore, the observer design problem in these systems is not much different from that in a system with any other type of input signal. However, in biological applications, the situation is quite different and impulsive control signals are often immeasurable, which circumstance poses a specific estimation problem. This class of system includes, among others, the pulsatile feedback in certain endocrine systems. In [2], a model for the non-basal testosterone regulation in the male, based on the concept of pulse-modulated feedback, is proposed.

*This research has been supported by the European Research Council (ERC) via the Advanced Grant 247035.

†P. Mattsson and A. Medvedev are with the department of Information Technology, Uppsala University, Uppsala, Sweden.

Continuous dynamic systems with intrinsic pulse-modulated feedback constitute a special class of hybrid systems where discrete states related to the modulation law are observed through continuous measurements. Thus, estimating the impulsive input signal to the continuous part can be viewed upon as estimation of a discrete state variable in a hybrid system.

Observability notions and observers for hybrid system, especially for those with switching continuous dynamics, have been considered in the literature, e.g. [3] and [4]. In [5], observers for impulsive systems where both the continuous-time dynamics and the resetting law is linear are considered. Unfortunately, most of existing approaches for designing hybrid observers fail when no measurements of the discrete state variables in a hybrid system are readily available.

A challenge in observing the states in an impulsive system is the fact that the states are reset after a finite time, and thus the Luenberger observer or Kalman filter will lose track of the state vector at every resetting event if the information about the moments of resetting are not provided. In [6] and [7], a static gain observer for a class of impulsive systems is studied, and local stability results for periodic solutions are proved. However, this observer typically exhibits slow convergence and can only be used when the resetting law (pulse-modulation law) is known.

The present paper considers impulsive systems with linear continuous dynamics and an unknown resetting law. As a solution to the problem of estimating the resetting events in the linear time-invariant dynamics, an approach making use of finite memory least-squares observers is considered.

The most widespread continuous least-squares observer, the L_2-optimal observer, see e.g. [8] p. 616, is known to be highly sensitive to structural uncertainties in the system parameters. However, in [9], a general framework for a class of least-squares observers is presented, and in [10] it is also proved to include the L_2-optimal observer as a special case. A least-squares observer yields, in theory, deadbeat estimation performance and, therefore, enables an exact estimate of the state vector in between resetting instants. In this paper, it is shown that this is the only information needed to determine the resetting events.

The paper is composed as follows. First the equations governing the class of impulsive systems under study are summarized. Then the finite memory least-squares observers are briefly reviewed and an estimation scheme for impulsive input signals is presented. Finally, a numerical example illustrating feasibility of the proposed technique is provided.

2 State Equations

Consider the impulsive dynamical system given by

$$\dot{x}(t) = Ax, \quad x(0) = x_o, \qquad t \notin \mathcal{T} \tag{1}$$
$$\Delta x(t) = g_k B, \qquad t = t_k \in \mathcal{T} \tag{2}$$
$$y(t) = Cx(t) \tag{3}$$

where

$$\begin{aligned} \Delta x(t) &= x(t^+) - x(t) \\ x(t^+) &= \lim_{\epsilon \to 0^+} x(t+\epsilon) = x(t) + g_k B, \end{aligned}$$

and $\mathcal{T}$ is a countable subset of $[0, \infty)$. To each $t_k \in \mathcal{T}$, there corresponds a $g_k \in \mathbb{R}$, called the impulse weight. The elements of $\mathcal{T}$ are assumed to be ordered so that $t_1 < t_2 < t_3 \ldots$. The square real $n \times n$ matrix A has distinct, non-zero eigenvalues and the matrix pair (A, C) is observable. The latter two assumptions on the process matrix are typically fulfilled in endocrine systems. The set $\mathcal{T}$ can be fixed, depend on the initial state, or be a realization of a stochastic process.

Equations (1) and (3) are referred to as the continuous-time dynamics and (2) as the resetting law. Note that (1)-(2) can be rewritten as

$$\dot{x}(t) = Ax + B\xi(t), \quad x(0) = x_o \tag{4}$$

where

$$\xi(t) = \sum_{t_k \in \mathcal{T}} g_k \delta(t - t_k),$$

and $\delta(\cdot)$ is the Dirac delta function. This reformulation explains why g_k is called the impulse weight but, however, recourses to theory of distributions.

Furthermore, the system is assumed to have a strictly positive minimum dwell time Φ, i.e.

$$0 < \Phi \leq t_{k+1} - t_k$$

for all k. This is also a standard assumption in pulse-modulated systems.

3 Continuous Least-Squares Observers

The conventional L_2-optimal observer, presented in e.g. [8], is given by the equation

$$\hat{x}_H(t) = \mathcal{W}_\tau^{-1} \int_{t-\tau}^{t} e^{A^T(\theta - t)} C^T y(\theta) d\theta \tag{5}$$

where

$$\mathcal{W}_\tau = \int_0^\tau e^{-A^T\theta} C^T C e^{-A\theta} d\theta$$

and yields a deadbeat state estimation performance, i.e. $\hat{x}_H(t) = x(t)$ for all $t \geq \tau$, in absence of resetting events. In [10], it is proved that observer (5) is contained in the following class of observers.

Let the operator $(P\cdot)(\lambda; t)$, depending on parameter $\lambda \in \Lambda$, be defined via the Laplace inversion integral

$$(Pv)(\lambda; t) = \frac{1}{2\pi j} \int_{c-j\infty}^{c+j\infty} p(\lambda, s) V(s) e^{st} ds \tag{6}$$

where $V(s)$ is the Laplace transform of $v(t)$, c is a suitable real constant and Λ is a nonempty finite real set. In the context of pseudodifferential operators, $p(\lambda, s)$ is called the symbol of the operator $(P\cdot)(\lambda; t)$. Along the lines of [9], consider the following observer

$$\hat{x}(t) = \mathcal{V}^{-1} \sum_{\lambda_i \in \Lambda} p(\lambda_i, A)^T C^T (Py)(\lambda_i; t) \tag{7}$$

where

$$\mathcal{V} = \sum_{\lambda_i \in \Lambda} p(\lambda_i, A)^T C^T C p(\lambda_i, A).$$

In this contribution, a particular finite-memory convolution operator

$$(Pv)(\lambda, \tau; t) = \int_{t-\tau}^{t} e^{\lambda(t-\theta)} v(\theta) d\theta \tag{8}$$

with the symbol

$$p(\lambda, \tau, s) = \frac{1 - e^{(\lambda - s)\tau}}{s - \lambda} \tag{9}$$

will be utilized. In general though, the choice of implementation operator in (7) is a design degree of freedom. So far, there has not been much work done on how to select or compute a "good" operator $p(\lambda, s)$. In fact, as demonstrated in [10], the L_2-optimal solution of the problem, where the optimal symbol can be obtained analytically, leads to a non-robust observer in case of stable plant dynamics.

Introduce the following notation

$$W(\lambda, \tau) = C \left(I - e^{(\lambda I - A)\tau} \right) (A - \lambda I)^{-1}, \tag{10}$$

$$Y(\lambda, \tau; t) = (Py)(\lambda, \tau; t). \tag{11}$$

Then observer (7) with operator (8) can be written as

$$\hat{x}_\tau(t) = \mathcal{V}_\tau^{-1} \sum_{\lambda_i \in \Lambda} W^T(\lambda, \tau) Y(\lambda, \tau; t) \tag{12}$$

where

$$\mathcal{V}_\tau = \sum_{\lambda_i \in \Lambda} W^T(\lambda_i, \tau) W(\lambda_i, \tau).$$

The following result formally establishes deadbeat performance of observer (12) for almost every set Λ.

Proposition 3.1. *Assume that Λ contains at least n distinct elements, $\Lambda \cap \sigma(A) = \emptyset$ and $\mathcal{T} \cap [t-\tau, t] = \emptyset$. For any observable pair (A, C) observer (12) possesses the following property: $\hat{x}_\tau(t) - x(t) \equiv 0$.*

Proof. See [11]. □

In what follows, Λ is assumed to contain at least n distinct elements and be disjoint with the spectrum of the matrix A, i.e.

$$\Lambda \cap \sigma(A) = \emptyset. \tag{13}$$

This assumption is not restrictive since the elements of Λ can always be selected to satisfy (13).

3.1 The observer parameters

Proposition 3.1 proves that (12) has deadbeat performance for almost every set Λ, but it does not give any suggestion as for how to choose the design parameters in practice. In [10], the sensitivity of (12) to uncertainty in the system matrix of the plant is studied using the Fréchet derivative. In [12] and [13], the effect of measurement noise on the observer estimate is studied, providing at least some insight into the choice of Λ.

In this section, the influence of the user parameters on the low-pass filter characteristics of $p(\lambda, \tau, s)$ is discussed. Consider

$$\bar{p}(\lambda, \tau, s) = \frac{\lambda}{e^{\lambda\tau} - 1} p(\lambda, \tau, s)$$

that is $p(\lambda, \tau, s)$ normalized so that the static gain is one. Define ω_b as the bandwidth of $\bar{p}(\lambda, \tau, s)$, i.e. the lowest frequency such that the inequality

$$|\bar{p}(\lambda, \tau, j\omega)| < \frac{1}{\sqrt{2}}, \quad \forall \omega > \omega_b$$

is satisfied. Then

$$|\bar{p}(\lambda,\tau,j\omega)|^2 = \frac{1+e^{2\lambda\tau}-2e^{\lambda\tau}\cos(\omega\tau)}{\omega^2+\lambda^2}\frac{\lambda^2}{(e^{\lambda\tau}-1)^2} \leq \frac{1+e^{2\lambda\tau}+2e^{\lambda\tau}}{\omega^2+\lambda^2}\frac{\lambda^2}{(e^{\lambda\tau}-1)^2} = \frac{\lambda^2}{\omega^2+\lambda^2}\coth^2(\lambda\tau/2)$$

and thus an upper bound for the bandwidth is

$$\omega_b \leq \bar{\omega}_b \triangleq \sqrt{\lambda^2(2\coth^2(\lambda\tau/2)-1)}.$$

For a fixed τ it can be shown that

$$\inf_{\lambda}\bar{\omega}_b = \lim_{\lambda\to 0}\sqrt{\lambda^2(2\coth^2(\lambda\tau/2)-1)} = \frac{2\sqrt{2}}{\tau}.$$

The above result suggests that observer (12) is better at filtering out high frequency noise when the elements of Λ are small and τ is large. However, in general, choosing all $\lambda_i \in \Lambda$ close to zero may lead to numerical problems. The choice of τ is also a trade-off, since the estimation delay increases with τ. Also, for the purposes of this paper, τ has to be less than the minimal dwell time Φ, see Section 4.

3.2 The effect of a resetting event on the observer

The observer (12) utilizes output measurements within the sliding window $[t-\tau, t]$ to estimate the state vector at time t. Due to Proposition 3.1, this estimate is exact when there is no resetting event within this window. However, as soon as a resetting event takes place in the scope of the window, the observer estimate will diverge from the true state vector.

Lemma 3.1. *Assume that* $\mathcal{T} \cap [t-\tau, t] = \{t_k\}$. *Then*

$$x(t) - \hat{x}_\tau(t) = g_k\left[I - \mathcal{V}_\tau^{-1}\sum_{\lambda_i\in\Lambda} W^T(\lambda_i,\tau)W(\lambda_i, t-t_k)\right]e^{A(t-t_k)}B$$

Proof. See Appendix A. □

4 Impulse Detection

In order to detect when a resetting event occurs, two observers of the form (12) with overlapping sliding windows can be used. A similar approach involving two deadbeat observers but for the purpose of fault detection has been suggested in [11].

Pick a set Λ that fulfills the conditions of Proposition 3.1 and choose the time delays τ_1 and τ_2 so that

$$0 < \tau_1 < \tau_2 < \Phi.$$

This particular choice of τ_1 and τ_2 ensures that there can be at most one resetting event in the time interval $[t - \tau_2, t]$.

Lemma 4.1. *For any choice of the time delays τ_1, τ_2 and an observable pair (A, C), there is a state-space realization of (1)-(3) such that*

$$\mathcal{V}_{\tau_1} = I, \quad \mathcal{V}_{\tau_2} = D \tag{14}$$

where D is a diagonal matrix with strictly positive elements.

Proof. See Appendix B. □

In what follows, it is assumed that the state vector in plant equations (1) is chosen so that (14) holds. This not only provides more compact notation but also optimizes the numerical properties of the underlying least-squares observers, [9].

Now introduce two observers $\hat{x}_{\tau_1}(t)$ and $\hat{x}_{\tau_2}(t)$, as in (12), but with different values of the sliding window width. The difference between the observers' estimates is called the state estimation residual and is denoted as

$$r(t) = \hat{x}_{\tau_1}(t) - \hat{x}_{\tau_2}(t)$$

It follows that $r(t) = 0$ when there is no resetting event within $[t - \tau_2, t]$, and that $r(t) \neq 0$ otherwise. Next, two ways to extract information about t_k and g_k from $r(t)$ are considered.

4.1 Integrating the state estimation residual

Assume that there is a resetting time $t_k \in [t-\tau, t]$, then for any $0 < \epsilon_1, \epsilon_2 < \Phi - \tau_2$, it holds that

$$R(t_k) \triangleq \int_{t_k}^{t_k+\tau_2} r(\theta)d\theta = \int_{t_k-\epsilon_1}^{t_k+\tau_2+\epsilon_2} r(\theta)d\theta. \tag{15}$$

Hence $R(t_k)$ can be computed without knowing exactly when the resetting event occurs. Also notice that

$$r(t) = -(x(t) - \hat{x}_{\tau_1}(t)) + (x(t) - \hat{x}_{\tau_2}(t)).$$

From the relations above and Lemma 3.1, it follows that $R(t_k)$ does not depend on the time t_k but only on the impulse weight g_k. The following proposition gives an explicit expression for this relationship.

Proposition 4.1. *If $t_k \in \mathcal{T}$ then*

$$\begin{aligned} R(t_k)/g_k = \\ &(e^{A\tau_2} - e^{A\tau_1})A^{-1}B \\ &+ \sum_{\lambda_i \in \Lambda} W^T(\lambda_i, \tau_1)K(\lambda_i, \tau_1)B \\ &- D^{-1} \sum_{\lambda_i \in \Lambda} W^T(\lambda_i, \tau_2)K(\lambda_i, \tau_2)B \end{aligned}$$

where

$$K(\lambda, \tau) = C\left[(e^{A\tau} - I)A^{-1} - \frac{1}{\lambda}(e^{\lambda\tau} - 1)I\right](A - \lambda I)^{-1}$$

Proof. See Appendix C □

Let the vectors a_k be defined by

$$a_0 = 0, \quad \text{and } a_k = R(t_k) + a_{k-1} \text{ for } k > 0.$$

Since $r(t) = 0$ for $t \in (t_k + \tau_2, t_{k+1})$, it follows that

$$a_k = \int_0^t r(\theta)d\theta$$

for all $k > 0$ and $t \in [t_k + \tau_2, t_{k+1}]$. When the output signal is corrupted by measurement noise, the constants a_k can be estimated by taking the mean value on an interval where the integral is nearly constant, see Section 5. Since

$$a_k - a_{k-1} = R(t_k)$$

and $R(t_k)/g_k$ is a known constant, the estimates of $a_k - a_{k-1}$ can be used to estimate g_k.

4.2 Estimating resetting times

Assume that the values of $Y(\lambda_j, \tau_2; t)$ are computed for at least two $\lambda_j \in \Lambda$ involved in the estimate $\hat{x}_{\tau_2}(t)$. Then the result of the following proposition can be used in order to estimate both t_k and g_k.

Proposition 4.2. *If $\mathcal{T} \cap [t - \tau_2, t] = \{t_k\}$ and $\mathcal{T} \cap [t - \tau_1, t] = \emptyset$ then*

$$\begin{aligned} g_k e^{(t-t_k)\lambda} C(\lambda I - A)^{-1}B = \\ Y(\lambda, \tau_2) - C(\lambda I - A)^{-1}(e^{\lambda\tau_2}\hat{x}_{\tau_1}(t - \tau_2) - \hat{x}_{\tau_1}(t)) \end{aligned} \quad (16)$$

Proof. See Appendix D. □

Note that the system with two unknowns t_k and g_k

$$\begin{cases} g_k e^{(t-t_k)\lambda_1} = f_1 \\ g_k e^{(t-t_k)\lambda_2} = f_2 \end{cases}$$

is uniquely solved by

$$\begin{cases} t_k = \frac{\ln(f_2)-\ln(f_1)}{\lambda_1-\lambda_2} + t \\ \\ g_k = f_1 e^{(t_k-t)\lambda_1} \end{cases}.$$

Since each row in (16) can be written in a similar manner, g_k and t_k can be evaluated exactly as long as $Y(\lambda_j, \tau_2; t)$ is computed for two distinct λ_j, which is the case considered below. However, it is also possible to compute $Y(\lambda_j, \tau_2; t)$ for all $\lambda_j \in \Lambda$, and solve the resulting overdetermined system of equations, e.g. using least-squares techniques. This can be implemented in the form of the algorithm below.

1. Start while $r(t)$ is zero.
2. Wait for $r(t)$ to become non-zero implying that a resetting event has occurred.
3. Wait for time τ_1. Now the expression in Proposition 4.2 holds.
4. Compute the right-hand side of (16) for at least two λ and solve for t_k and g_k, or use estimates of g_k and solve only for t_k.

Note that it is not necessary to obtain the exact time when $r(t)$ becomes non-zero. In fact, it suffices that Step 3 of the algorithm is performed at a time $t \in (t_k + \tau_1, t_k + \tau_2)$. Thus, in order to reduce sensitivity to noise, one can carry out Step 3 for several instants t and then use the mean value as an estimate. Logically, the check for a non-zero state estimate residual in Step 1 can be replaced by a check against a suitable threshold.

5 Numerical Example

In this section, the proposed techniques for impulsive input estimation are validated on a numerical example.

Assume the following values in model (1)-(3)

$$A = \begin{bmatrix} -0.1 & 0 \\ 0.8 & -0.014 \end{bmatrix}, \qquad B = \begin{bmatrix} 1 \\ 0 \end{bmatrix}$$

$$C = \begin{bmatrix} 0 & 1 \end{bmatrix}, \qquad x_o^T = \begin{bmatrix} 0 & 0 \end{bmatrix}$$

with four impacting delta-functions at the time instants $\mathcal{T} = \{5, 80, 160, 230\}$ and with the weights $g_1 = 0.8$, $g_2 = 0.9$, $g_3 = 0.6$ and $g_4 = 0.7$. To evaluate the performance of the estimation algorithms under measurement noise, zero mean white noise with variance 0.1 is added to the output of (1)-(3). The output of the plant with noise is shown in Fig. 1.

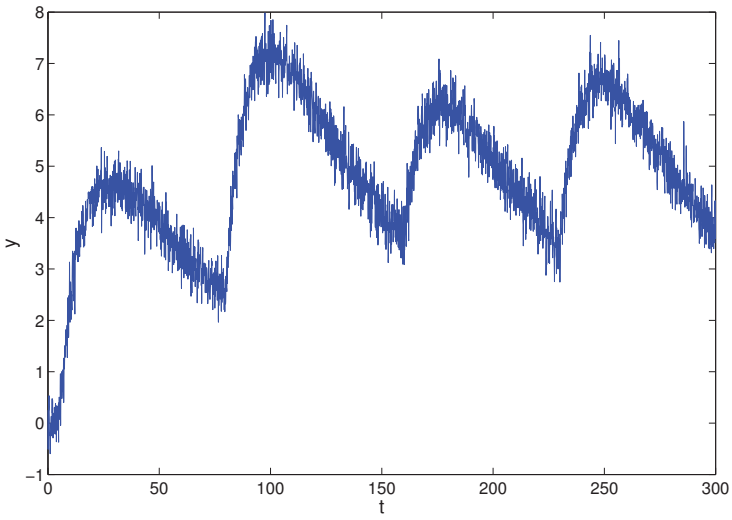

Figure 1: The output signal with measurement noise

For the observer, the time delays are assigned as $\tau_1 = 30$ and $\tau_2 = 50$, while $\Lambda = \{-0.03, -0.08\}$. Balancing the state-space description with the transformation $x \to Tx$

$$T = \begin{bmatrix} -758.49 & 27.13 \\ 163.24 & -1.45 \end{bmatrix},$$

makes the system satisfy (14) with

$$D = \begin{bmatrix} 0.18 & 0 \\ 0 & 597.39 \end{bmatrix}.$$

Choosing the elements of Λ closer to zero would reduce the impact of the noise, but would also probably lead to a larger condition number of D.

For the balanced system, the expression on the right-hand side in Proposition 4.1 is

$$\frac{R(t_k)}{g_k} = \begin{bmatrix} -354.85 \\ 192.24 \end{bmatrix} \tag{17}$$

From the discussion in Section 4.1, it follows that the integral of $r(t)$ in the noise-free case is constant on the intervals $(t_k + \tau_2, t_{k+1})$. The integral of $r(t)$

corrupted by noise can be seen in Fig. 2. The constants a_k are approximated by taking the mean of the red parts in Fig. 2, resulting in the estimated values

$$\hat{a}_1 = \begin{bmatrix} -282.99 \\ 152.99 \end{bmatrix}, \quad \hat{a}_2 = \begin{bmatrix} -602.17 \\ 326.25 \end{bmatrix}$$
$$\hat{a}_3 = \begin{bmatrix} -814.32 \\ 441.11 \end{bmatrix}, \quad \hat{a}_4 = \begin{bmatrix} -1062.3 \\ 575.52 \end{bmatrix}.$$

Let G_k be the result of element-wise division of $\hat{a}_k - \hat{a}_{k-1}$ by the right-hand side of (17). Taking the mean of the elements in G_k as estimates for g_k gives

$$\hat{g}_1 = 0.7955, \quad \hat{g}_2 = 0.9016, \quad \hat{g}_3 = 0.5977, \quad \hat{g}_4 = 0.6990$$

Next both the resetting times t_k and the impulse weights g_k are estimated

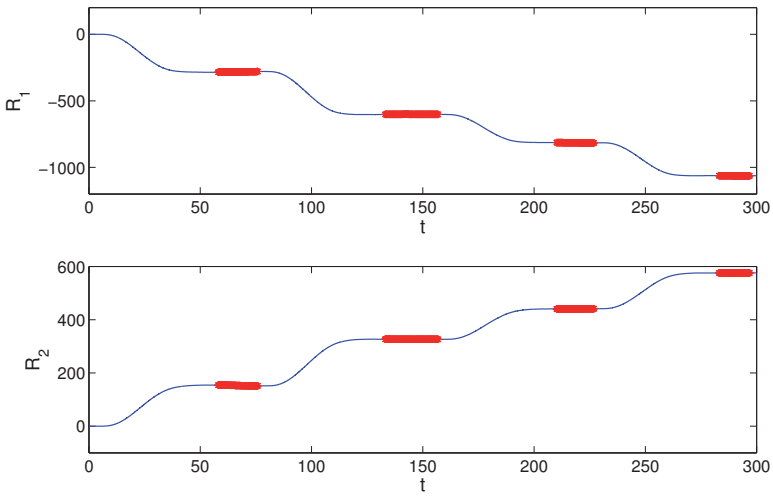

Figure 2: The integral of $r(t)$. The parts marked with a red line are used to compute g_k.

using the procedure in Section 4.2. The function $r(t)$ is plotted in Fig. 3. In an attempt to decrease the sensitivity to noise, the right hand side of (16) has been computed for all t marked by a red line in Fig. 3. This gives an estimate of g_k and t_k for each t, and taking the mean value of all these estimates gives

$$\hat{t}_1 = 5.22, \quad \hat{t}_2 = 80.06, \quad \hat{t}_3 = 159.87, \quad \hat{t}_4 = 230.12$$

and

$$\hat{g}_1 = 0.8101, \quad \hat{g}_2 = 0.9104, \quad \hat{g}_3 = 0.5937, \quad \hat{g}_4 = 0.6968.$$

The estimates of g_k using this method are slightly worse than those for the integration method, but here estimates of the resetting times t_k are also given.

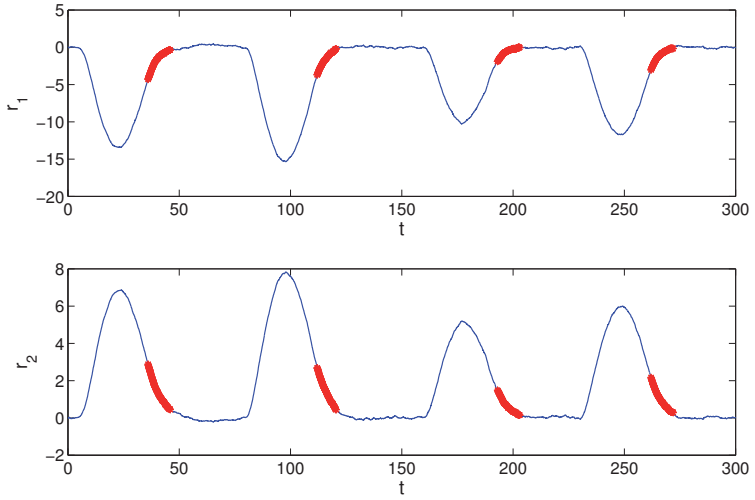

Figure 3: The state estimation residual $r(t)$.

6 Conclusion

An observer-based procedure for the estimation of firing times and weights of Dirac delta-functions impacting a continuous linear time-invariant system is suggested. The core of the method is in the use of continuous least-squares observers implemented by means of a finite memory convolution operator. A numerical example demonstrates the feasibility of the proposed estimation scheme that is expected to be useful in detecting instants and weights of pulsatile events in non-basal endocrine secretion.

References

[1] W. M. Haddad, V. Chellaboina, and S. G. Nersesov, *Impulsive and Hybrid Dynamical Systems: Stability, Dissipativity, and Control*. Princeton: Princeton Univ. Press, 2006.

[2] A. Churilov, A. Medvedev, and A. Shepeljavyi, "Mathematical model of non-basal testosterone regulation in the male by pulse modulated feedback," *Automatica*, vol. 45, no. 1, pp. 78–85, 2009.

[3] A. Balluchi, L. Benvenuti, M. Di Benedetto, and A. Sangiovanni-Vincentelli, "Design of observers for hybrid systems," in *Hybrid Systems: Computation and Control*, ser. Lecture Notes in Computer Science, C. Tomlin and M. Greenstreet, Eds. Springer Berlin / Heidelberg, 2002, vol. 2289, pp. 59–80.

[4] A. Alessandri and P. Coletta, "Switching observers for continuous-time and discrete-time linear systems," in *American Control Conference, 2001. Proceedings of the 2001*, vol. 3, 2001, pp. 2516 –2521 vol.3.

[5] E. Medina and D. Lawrence, "State estimation for linear impulsive systems," in *American Control Conference, 2009. ACC '09.*, june 2009, pp. 1183 –1188.

[6] A. Churilov, A. Medvedev, and A. Shepeljavyi, "State observer for continuous oscillating systems with pulsatile feedback," in *IFAC World Congress*, Milano, Italy, September 2011, accepted for presentation.

[7] ——, "Further results on a state observer for continuous oscillating systems under intrinsic pulsatile feedback," in *IEEE Conference on Decision and Control*, Orlando, FL, December 2011, accepted for presentation.

[8] T. Kailath, *Linear Systems*. Englewood Cliffs, N.J.: Prentice-Hall, Inc., 1980.

[9] A. Medvedev, "Continuous least-squares observers with applications," *IEEE Transactions on Automatic Control*, vol. 41, pp. 1530–1536, 1996.

[10] A. Medvedev and H. T. Toivonen, "Directional sensitivity of continuous least-squares state estimators," *Systems & Control Letters*, vol. 59, no. 9, pp. 571–577, 2010.

[11] A. Medvedev, "State estimation and fault detection by a bank of continuous finite-memory filters," *International Journal of Control*, vol. 69, no. 4, pp. 499–517, 1998.

[12] M. Bask and A. Medvedev, "Analysis of least-squares state estimators for a harmonic oscillator," in *Decision and Control, 2000. Proceedings of the 39th IEEE Conference on*, vol. 4, 2000, pp. 3819 –3824 vol.4.

[13] A. Medvedev, "Disturbance attenuation in finite-spectrum-assignment controllers," *Automatica*, vol. 33, no. 6, pp. 1163 – 1168, 1997.

A Proof of Lemma 3.1

Assume $\mathcal{T} \cap [t-\tau, t] = \{t_k\}$, and let $x_o = x(t-\tau)$. Then the state vector is given by

$$x(\theta) = \begin{cases} e^{A(\theta-t+\tau)}x_o & \text{if } \theta \in [t-\tau, t_k) \\ e^{A(\theta-t+\tau)}x_o + g_k e^{A(\theta-t_k)}B & \text{if } \theta \in (t_k, t] \end{cases}$$

Thus

$$\begin{aligned} Y(\lambda,\tau;t) &= \int_{t-\tau}^{t} e^{\lambda(t-\theta)}Cx(\theta)d\theta \\ &= \int_{t-\tau}^{t} e^{\lambda(t-\theta)}Ce^{A(\theta-t+\tau)}x_o d\theta + g_k \int_{t_k}^{t} e^{\lambda(t-\theta)}Ce^{A(\theta-t_k)}Bd\theta. \end{aligned}$$

Both integrals on the right-hand side can be written as

$$\int_a^t e^{\lambda(t-\theta)}Ce^{A(\theta-a)}zd\theta = C[e^{A(t-a)} - e^{\lambda I(t-a)}](A-\lambda I)^{-1}z = W(\lambda, t-a)e^{A(t-a)}z$$

hence

$$Y(\lambda,\tau;t) = W(\lambda,\tau)e^{A\tau}x_o + W(\lambda, t-t_k)e^{A(t-t_k)}g_k B$$

and

$$\hat{x}_\tau(t) = \mathcal{V}_\tau^{-1}\sum_{\lambda_i\in\Lambda} W^T(\lambda_i,\tau)Y(\lambda_i,\tau) = e^{A\tau}x_o + \mathcal{V}_\tau^{-1}\sum_{\lambda_i\in\Lambda} W^T(\lambda_i,\tau)W(\lambda_i, t-t_k)g_k e^{A(t-t_k)}B.$$

From this, and the fact that

$$x(t) = e^{A\tau}x_o + g_k e^{A(t-t_k)}B$$

the result of the proposition follows.

B Proof of Lemma 4.1

Let $\mathcal{V}_{\tau_1}$ and $\mathcal{V}_{\tau_2}$ correspond to the original system. A state transformation $\bar{x} = Tx$ results in

$$\bar{\mathcal{V}}_{\tau_1} = T^{-T}\mathcal{V}_{\tau_1}T^{-1}, \quad \bar{\mathcal{V}}_{\tau_2} = T^{-T}\mathcal{V}_{\tau_2}T^{-1}.$$

A transformation T such that $\bar{\mathcal{V}}_{\tau_1} = I$ and $\bar{\mathcal{V}}_{\tau_2} = D$ can be found in the following way. Since $\mathcal{V}_{\tau_1}$ is symmetric and positive definite there is an orthogonal U and diagonal L such that

$$\mathcal{V}_{\tau_1}^{-1} = ULU^T.$$

Let $T_1 = L^{-1/2}U^T$ and $\bar{\mathcal{V}} = T_1\mathcal{V}_{\tau_2}^{-1}T_1^T$. $\bar{\mathcal{V}}$ is symmetric and positive definite, so there exists an orthogonal V and a diagonal D such that

$$\bar{\mathcal{V}} = VD^{-1}V^T.$$

Now set $T = V^T L^{-1/2}U^T$. Then

$$\bar{\mathcal{V}}_{\tau_1} = T^{-T}\mathcal{V}_{\tau_1}T^{-1} = I$$

and

$$\bar{\mathcal{V}}_{\tau_2} = T^{-T}\mathcal{V}_{\tau_2}T^{-1} = D.$$

C Proof of Proposition 4.1

By direct integration it can be verified that

$$K(\lambda,\tau) = \int_{t_k}^{t_k+\tau} W(\lambda, t-t_k)e^{A(t-t_k)}dt$$

for any t_k. Using Lemma 3.1 it can also be seen that

$$\begin{aligned}\int_{t_k}^{t_k+\tau_j} (x(t) - \hat{x}_{\tau_j}(t))dt = \\ g_k \int_{t_k}^{t_k+\tau_j} e^{A(t-t_k)}dtB - g_k\mathcal{V}_{\tau_j}^{-1}\sum_{\lambda_i\in\Lambda} W^T(\lambda_i,\tau_j)K(\lambda_i,\tau_j)dtB = \\ g_k\left[(e^{A\tau_j} - I)A^{-1} - \mathcal{V}_{\tau_j}^{-1}\sum_{\lambda_i\in\Lambda} W^T(\lambda_i,\tau_j)K(\lambda_i,\tau_j)\right]B\end{aligned}$$

Inserting the equation above into

$$\int_{t_k}^{t_k+\tau_2} r(t)dt = \int_{t_k}^{t_k+\tau_2} \left[-(x(t) - \hat{x}_{\tau_1}(t)) + (x(t) - \hat{x}_{\tau_2}(t))\right]dt$$

proves the proposition.

D Proof of Proposition 4.2

Since $\mathcal{T} \cap [t-\tau_2, t] = \{t_k\}$ it follows, by the same reasoning as in Appendix A, that

$$\begin{aligned} Y(\lambda, \tau_2; t) = \\ & W(\lambda, \tau_2) e^{A\tau_2} x(t-\tau_2) + g_k W(\lambda, t-t_k) e^{A(t-t_k)} B = \\ & C(A-\lambda I)^{-1} \left(e^{A\tau_2} - e^{\lambda I \tau_2} \right) x(t-\tau_2) + \\ & C(A-\lambda I)^{-1} g_k \left(e^{A(t-t_k)} - e^{\lambda I (t-t_k)} \right) B \end{aligned}$$

Noticing that

$$x(t) = e^{A\tau_2} x(t-\tau_2) + g_k e^{A(t-t_k)} B$$

then gives

$$Y(\lambda, \tau_2; t) = C(\lambda I - A)^{-1} \left[g_k e^{\lambda(t-t_k)} B + e^{\lambda \tau_2} x(t-\tau_2) - x(t) \right].$$

This together with the fact that $\hat{x}_{\tau_1}(t-\tau_2) = x(t-\tau_2)$, $\hat{x}_{\tau_1}(t) = x(t)$ when $\mathcal{T} \cap [t-\tau_2, t] = \{t_k\}$ and $\mathcal{T} \cap [t-\tau_1, t] = \emptyset$ completes the proof.

Paper II

State Estimation in Linear Time-Invariant Systems With Unknown Impulsive Inputs

Per Mattsson and Alexander Medvedev*†

Abstract

This paper deals with state estimation in linear time-invariant systems subject to unknown impulsive input signals. A solution based on a linear impulsive observer and a finite-memory convolution operator is suggested. The problem arises e.g. in the context of systems with intrinsic pulse-modulated feedback that have recently been applied to mathematical modeling of endocrine systems with pulsatile hormone secretion. Simulation results illustrating the performance of the proposed method are provided.

1 Introduction

Mathematical models of dynamical systems with impulsive input signals appear often in mechanics, power electronics and biology, see e.g. [1], mostly in the applications where impulses represent external momentaneous interaction. In engineered systems, impulsive control signals are typically known and therefore can be taken into account in a similar manner as non-impulsive ones. For instance, observer design for this kind of systems is not much different from that in a system with any other kind of input signal.

However, in biological applications, the impulsive control signal is often unknown. A characteristic example of this class of systems is presented by the pulsatile endocrine feedback [2]. In [3], a mathematical model for the non-basal testosterone regulation in the male, based on the concept of pulse-modulated feedback, is proposed and investigated.

A challenge in devising observers for a system with unknown impulsive input signal is that the state variables are reset after a finite time. Thus, most classical asymptotic observers, such as the Luenberger observer [4], lose

*This research has been supported by the European Research Council (ERC) via the Advanced Grant 247035 and Grant 2012-3153 from the Swedish Research Council.

†P. Mattsson and A. Medvedev are with Information Technology, Uppsala University, Uppsala, Sweden.

track of the state vector after an impulse. A similar phenomenon occurs with respect to state estimation in switching system, when the switching time is unknown, as discussed in e.g. [5]. Impulsive observers can be utilized to deal with the state reset problem in impulsive systems.

An impulsive observer that finds the true state in finite time when the input is known is presented in [6], and a similar approach is used to implement observer-based control for systems with persistently acting impulsive input in [7]. In [8], observers for impulsive systems with linear continuous-time dynamics and a linear resetting law are considered. Further, in [9] and [10], a static gain observer for linear continuous systems under intrinsic impulsive feedback is studied, and conditions for local stability of the observer under periodic solutions in the plant are proved.

Unfortunately, most of the existing approaches for designing an impulsive observer fail when there is no information about the input impulses. To fill this gap, an approach to the estimation of impulse times and weights by means of continuous least-squares observers is suggested in [11].

The present paper considers impulsive systems with linear continuous dynamics and unknown input impulses. As a solution to the state estimation problem, a method based on a linear observer coupled with an impulse estimation algorithm, similar to the one in [11], is considered.

The paper is composed as follows. First the equations governing the class of systems in hand are summarized. Then a general outline of the observer equations and impulse estimation algorithm is provided, followed by a more detailed explanation of each step. Finally, a numerical example illustrating the behaviour of the observer is given.

2 System Equations and Assumptions

Consider the (hybrid) dynamical system with state resets

$$\frac{dx}{dt} = Ax\,, \qquad t \notin \mathcal{T} \tag{1}$$

$$\Delta x(t) = g_k B\,, \qquad t = t_k \in \mathcal{T} \tag{2}$$

$$y(t) = Cx(t), \tag{3}$$

where

$$\Delta x(t) = x(t^+) - x(t),$$
$$x(t^+) = \lim_{\epsilon \to 0^+} x(t+\epsilon) = x(t) + g_k B,$$

and $\mathcal{T}$ is a countable subset of $[0, \infty)$, where t_k are assumed to be ordered so that $t_1 < t_2 < t_3 < \ldots$.

The instants t_k are called impulse times, and to each impulse time, there is a corresponding impulse weight $g_k \in \mathbb{R}$. Notice that negative weights are allowed in this formulation. Equations (1)-(2) can be equivalently rewritten as

$$\dot{x}(t) = Ax + B\xi(t),$$

where

$$\xi(t) = \sum_{t_k \in \mathcal{T}} g_k \delta(t - t_k),$$

and $\delta(\cdot)$ is the Dirac delta function. This reformulation clarifies why t_k, g_k are called impulse time and weight, respectively.

It is assumed that the system has a minimum dwell time Φ, i.e.

$$0 < \Phi \leq t_{k+1} - t_k$$

for all k. This is a standard assumption in pulse-modulated systems. In biological systems, it is typically motivated by the time required for an organ or cell to recuperate.

Furthermore, it is assumed that A is a real $n \times n$ matrix, C is a real row vector, B is a real column vector and the matrix pair (A, C) is observable. It can be noted that the observer presented in this paper can easily be extended to also handle known inputs and more than one output.

3 The Observer

In order to estimate the state vector of (1), the impulsive observer

$$\frac{d\hat{x}}{dt} = A\hat{x} + K(y - \hat{y}), \qquad t \notin \hat{\mathcal{T}} \tag{4}$$

$$\Delta\hat{x}(t) = \hat{g}_l B, \qquad t = \hat{t}_l \in \hat{\mathcal{T}} \tag{5}$$

$$\hat{y}(t) = C\hat{x}(t) \tag{6}$$

will be used, where $\hat{t}_l, \hat{g}_l$ are refereed to as the observer impulse times and weights respectively. Let

$$D = A - KC.$$

It is assumed that the observer gain K is chosen so that D is Hurwitz stable with distinct eigenvalues. Notice that, since (A, C) is observable, it follows that (D, C) is observable too.

The state estimation error $\varepsilon(t) = x(t) - \hat{x}(t)$ is governed by the equations

$$\frac{d\varepsilon}{dt} = D\varepsilon, \qquad t \notin \mathcal{T} \cup \hat{\mathcal{T}}, \tag{7}$$

$$\Delta\varepsilon(t) = g_k B, \qquad t = t_k \in \mathcal{T}, \tag{8}$$

$$\Delta\varepsilon(t) = -\hat{g}_l B, \qquad t = \hat{t}_l \in \hat{\mathcal{T}}. \tag{9}$$

If the impulses in the plant are known, then the observer impulses could be chosen so that $\hat{t}_k = t_k$ and $\hat{g}_k = g_k$. In this case the state estimation error for $t \geq 0$ is given by $\varepsilon(t) = e^{Dt}\varepsilon(0)$.

However, in the case investigated in the present paper, the plant impulses are unknown. To solve the problem with unknown impulses, it is assumed that, at any time t, the future output values $y(\cdot)$ within a sliding window $y(\theta), \theta \in [t, t+\tau)$ are made available to the observer. This is possible e.g. if the observer is run off-line or the state estimates are allowed to be delayed τ time units. A periodic mode in the plant (as in [9]) also opens up for an application of the present technique. Furthermore, it is assumed that $\tau < \Phi$, so that there is at most one plant impulse in the sliding window at any time t.

At time t, the observer will utilize a finite-memory convolution operator on the output $y(\theta)$, $\theta \in [t, t+\tau)$, to decide whether or not an observer impulse should be added in the current interval. If so, the same operator is used to evaluate the observer impulse time and weight.

3.1 Impulsive observer algorithm

A general outline of the algorithm is given next with the details provided in the subsequent sections.

1. Propagate the observer according to (4), until the condition for adding an observer impulse is met (see Section 3.3). Let t_o be the time when the condition was met.

2. Determine the observer impulse time $\hat{t}_l \in [t_o, t_o + \tau)$ and weight $\hat{g}_l$. (See Section 3.4.)

3. Propagate the observer according to (4)-(5), until $t = t_o + \tau$.

4. Go to Step 1.

3.2 The finite-memory convolution operator

In this contribution, the finite-memory convolution operator

$$(Pf)(\lambda, \tau; t) = \int_{t-\tau}^{t} e^{\lambda(t-\theta)} f(\theta) d\theta \tag{10}$$

will be utilized. In virtue of being a pseudodifferential operator, $(Pf)(\lambda, \tau; t)$ is characterized by the symbol

$$p(\lambda, \tau, s) = \frac{1 - e^{(\lambda - s)\tau}}{s - \lambda}, \tag{11}$$

so that

$$\mathcal{L}\{(Pf)(\lambda,\tau;t)\} = p(\lambda,\tau,s)F(s),$$

where $\mathcal{L}\{\cdot\}$ denotes the Laplace transform and $F(s) = \mathcal{L}\{f(t)\}$. This operator has previously been used for e.g. exact (deadbeat) state estimation, see e.g. [12], finite spectrum assignment control of time-delay systems [13], and also impulse detection [11].

Notice that the symbol in (11) can also be employed for defining a matrix function, i.e. for a square matrix M

$$p(\lambda,\tau,M) = \left(I - e^{(\lambda I - M)\tau}\right)(M - \lambda I)^{-1}.$$

Let $\Lambda = \{\lambda_1,\ldots,\lambda_m\}$ be a set of real and distinct elements, and introduce the following notation

$$W(t) \triangleq \begin{bmatrix} Cp(\lambda_1,t,D) \\ \vdots \\ Cp(\lambda_m,t,D) \end{bmatrix}.$$

Also let $\mathcal{V} = W^T(\tau)W(\tau)$ and

$$V(t) = W(t)e^{Dt}.$$

In what follows, Λ is assumed to contain at least n distinct elements and be disjoint from the spectrum of the matrix D, i.e.

$$\Lambda \cap \sigma(D) = \emptyset, \tag{12}$$

where $\sigma(D)$ is the spectrum of D. This assumption is not restrictive since the elements of Λ can always be selected to satisfy the condition above.

Assumption (12) also implies that $\mathcal{V}$ is positive definite, so that a weighted vector norm

$$\|x\|_{\mathcal{V}}^2 = \|W(\tau)x\|^2 = x^T\mathcal{V}x$$

can be introduced together with the usual Euclidean one: $\|x\|^2 = x^Tx$. It is straightforward to show (see e.g. [11]) that given the set Λ, it is possible to find a nonsingular state transformation matrix T, such that $\mathcal{V}$ for the transformed system and observer is equal to the identity matrix and resulting in $\|x\| = \|x\|_{\mathcal{V}}$.

In order to choose the observer impulses, operator (10) will be applied to the output error $\bar{y}(t)$ that would be present if there were no observer impulse after some time t_o. That is

$$\bar{y}(t) = C\bar{\varepsilon}(t),$$

where $\bar{\varepsilon}(t)$ is the solution to (7)-(8) with the initial value $\bar{\varepsilon}(t_o) = \varepsilon(t_o)$. Define

$$R(t_o) \triangleq \begin{bmatrix} (P\bar{y})(\lambda_1, \tau; t_o + \tau) \\ \vdots \\ (P\bar{y})(\lambda_m, \tau; t_o + \tau) \end{bmatrix}. \tag{13}$$

Notice that $\bar{y}(t)$, and thus $R(t_o)$, can be computed if $\hat{x}(t_o)$ is known together with the output $y(t)$ for $t \in [t_o, t_o + \tau)$.

Proposition 3.1. *If $\mathcal{T} \cap [t_o, t_o + \tau) = \{t_k\}$, then*

$$R(t_o) = V(\tau)\varepsilon(t_o) + g_k V(t_o + \tau - t_k)B,$$

and if $\mathcal{T} \cap [t_o, t_o + \tau) = \emptyset$, then

$$R(t_o) = V(\tau)\varepsilon(t_o).$$

Proof. Cf. Appendix I in [11]. □

Proposition 3.1 shows in what way $R(t)$ is affected when a plant impulse enters the sliding window $[t, t + \tau)$. It is also of interest to see how $R(t)$ is related to the state estimation error $\varepsilon(t)$.

Proposition 3.2. *Assume that $\mathcal{T} \cap [t_o, t_o + \tau) = \{t_k\}$ and $\hat{\mathcal{T}} \cap [t_o, t_o + \tau) = \{\hat{t}_l\}$. Then*

$$\begin{aligned} W(\tau)\varepsilon(t_o + \tau) &= V(\tau)\varepsilon(t_o) \\ &+ g_k \left(V(t_o + \tau - t_k)B + E(t_k - t_o)\right) \\ &- \hat{g}_l \left(V(t_o + \tau - \hat{t}_l)B + E(\hat{t}_l - t_o)\right), \end{aligned} \tag{14}$$

where

$$E(t) = (W(\tau) - W(\tau - t))e^{D(\tau - t)}B.$$

Furthermore, for any $\epsilon, r > 0$, it is possible to choose the set Λ such that each row of $V(t_o + \tau - \hat{t})B$ and $E(\hat{t} - t_o)$ satisfy

$$|E_i(\hat{t} - t_o)| \leq r|V_i(t_o + \tau - \hat{t})B|$$

when $\hat{t} - t_o \leq \tau - \epsilon$.

Proof. See Appendix A. □

Proposition 3.2 justifies the following important approximation. If Λ is chosen such that the proposition holds for a small enough r, and there are no impulses in $[t_o + \tau - \epsilon, t_o + \tau)$, then the terms $g_k E(t_k - t_o)$ and $\hat{g}_l E(\hat{t}_l - t_o)$ in (14) are negligible. Thus it follows from Proposition 3.1 that

$$W(\tau)\varepsilon(t_o + \tau) \approx R(t_o) - \hat{g}_l V(t_o + \tau - \hat{t}_l). \tag{15}$$

3.3 Step 1: Deciding on observer impulse

This section deals with the first step in the impulsive observer algorithm of Section 3.1. In this step, the observer propagates the state estimation $\hat{x}(t)$ according to (4) and computes $R(t)$, defined in (13), for each t. This continues until some time t_o, when it is decided that there should be an observer impulse in the interval $[t_o, t_o + \tau)$.

In order to see whether or not an observer impulse should be added, $\|R(t)\|$ will be considered. Notice that if $\varepsilon(t) = 0$ and $\mathcal{T} \cap [t, t + \tau) = \emptyset$, then it follows from Proposition 3.1 that $R(t) = 0$. However, as soon as an impulse at t_k enters the sliding window $[t, t+\tau)$, the norm of $R(t)$ will start to increase according to the relationship

$$\|R(t)\| = |g_k| \, \|V(t + \tau - t_k)B\| \,, \quad 0 < t_k - t < \tau. \tag{16}$$

Thus, if $\|R(t)\| > 0$, then $\varepsilon(t) \neq 0$ and/or $\mathcal{T} \cap [t, t + \tau) \neq \emptyset$. In both cases, there is a reason to add an observer impulse. If $\varepsilon(t_o) \neq 0$, then the observer impulse could be used to reduce the state estimation error, and if there is a plant impulse within $[t, t + \tau)$, then the observer should counter it with an observer impulse.

Thus, a condition for choosing t_o is that $\|R(t_o)\| > 0$. For robustness sake, zero in the right-hand side of the inequality can be replaced by

$$\|R(t_o)\| > \eta,$$

for some threshold $\eta > 0$.

It is also desirable, as motivated in Section 3.4, that (15) holds at time t_o. Due to Proposition 3.2, it is thus preferable to choose t_o so that there is no plant impulse in $[t_o + \tau - \epsilon, t_o + \tau)$, and the designer should take this into account when picking η.

Since the way in which $\|R(t)\|$ is affected by an impulse is known beforehand, this is usually not a problem, at least when some bounds on $|g_k|$ are known. For instance, the interval of admissible impulse weights is always known in pulse-modulated control. Notice that if $|g_k| \leq g_M$ for all k, then η could be chosen so that

$$\eta > g_M \left\| V(\tau - \hat{t})B \right\| , \quad \text{for } \tau - \epsilon < \hat{t} < \tau,$$

cf. (16). However, if η is chosen too large, small impulses might be missed.

It is often possible to devise a more advanced condition for choosing t_o, by studying the graph of

$$\|V(\tau - t_k)B\| \,, \quad 0 < t_k < \tau.$$

In this way it might be possible to choose t_o in a way that does not depend on the impulse weights. An example of this is provided in Section 4.

3.4 Step 2: Evaluating the observer impulse

This section deals with the second step in the impulsive observer algorithm of Section 3.1.

Suppose that it has been decided at time t_o that there should be an observer impulse in $[t_o, t_o + \tau)$, see Section 3.3. Let $\varepsilon_o = \varepsilon(t_o)$. Assume also that there is a plant impulse with weight g_k at time $t_k \in [t_o, t_o + \tau)$. If this is not the case, then $g_k = 0$ throughout this section.

When $\varepsilon_o = 0$, it follows from Proposition 3.1 that t_k and g_k can be found by solving

$$R(t_o) = \hat{g}_l V(t_o + \tau - \hat{t}_l)B. \tag{17}$$

However, for $\varepsilon_o \neq 0$, the above equation may not have a solution. Therefore, the following optimization problem is solved instead

$$\begin{aligned} \min_{\hat{t}_l, \hat{g}_l} \quad & \left\| R(t_o) - \hat{g}_l V(t_o + \tau - \hat{t}_l)B \right\|^2, \\ \text{s.t} \quad & t_o < \hat{t}_l < t_o + \tau. \end{aligned} \tag{18}$$

A suitable technique for solving this problem is discussed in Section 3.5.

For $\varepsilon_o = 0$, (17) is always satisfied by choosing $\hat{t}_l = t_k$ and $\hat{g}_l = g_k$. Numerical experiments indicate that this solution is also unique, but this result is not formally proved here.

To analyze what happens when $\varepsilon_o \neq 0$, assume that an observer impulse is fired at $\hat{t}_l$. If Λ has been chosen so that Proposition 3.2 holds for a small enough r, and there is no impulse in $[t_o + \tau - \epsilon, t_o + \tau)$ (see Section 3.3), then it can be concluded from (15) that

$$\|\varepsilon(t_o + \tau)\|_{\mathcal{V}}^2 \approx \left\| R(t_o) - \hat{g}_l V(t_o + \tau - \hat{t}_l)B \right\|^2. \tag{19}$$

The right-hand side of (19) is exactly the quantity that is minimized in (18). Also note that thanks to the minimization,

$$\left\| R(t_o) - \hat{g}_l V(t_o + \tau - \hat{t}_l)B \right\| \leq \left\| e^{D\tau}\varepsilon_o \right\|_{\mathcal{V}}.$$

Hence, if $\varepsilon_o \neq 0$, the observer might add an impulse that does not correspond to an impulse in the plant. However, in this case the "false" impulse is chosen so that

$$\|\varepsilon(t_o + \tau)\|_{\mathcal{V}} \lesssim \left\| e^{D\tau}\varepsilon_o \right\|_{\mathcal{V}}$$

where the right-hand side is the state estimation error that is acquired when the observer impulse coincides with the plant impulse.

In practice, the observer usually adds "false" impulses when the state estimation error is large, resulting in a faster convergence (see also Section 4). As the state estimation error decays over time, the observer impulses will get closer to the true plant impulses, as seen in Section 4.

3.5 Solving the optimization problem

Solving optimization problem (18) is an important part of the observer described above. Notice that the cost function depends linearly on $\hat{g}_l$. It follows that, if the pair $\hat{t}_l, \hat{g}_l$ minimizes the cost function in (18) then

$$\hat{g}_l = (B^T V^T V B)^{-1} B^T V^T R(t_o),$$

where $V = V(t_o + \tau - \hat{t}_l)$. Inserting this into (18) gives rise to a nonlinear optimization problem in one variable. Thanks to the constraint $\hat{t}_l \in [t_o, t_o + \tau)$, this problem can be solved with an arbitrary accuracy by gridding the interval, evaluating the cost function at each point, and selecting the solution that corresponds to the least cost function value.

3.6 The observer parameters

Besides the condition discussed in Section 3.3 (e.g. choosing the threshold η), the designer has to choose the observer gain matrix K, the length of the sliding window τ, and the set Λ.

The proof of Proposition 3.2 shows that letting the elements of Λ tend to negative infinity ensures that the approximation in (15) is valid. However, other aspects have also to be taken into account. In [13] and [11], the low-pass characteristics and disturbance attenuation of the operator (10) are studied. It is demonstrated that the operator in general is less sensitive to measurement noise when $|\lambda|$ is small. Thus there is a trade-off between making r in Proposition 3.2 small, and decreasing the sensitivity to noise. Fortunately, this trade-off can usually be handled in practice, as shown in Section 4. It is also seen that the sensitivity to high frequency noise is reduced when τ is increased. However, increasing τ leads to a longer lag in the state estimate. Furthermore, τ must be chosen less than Φ, which limitation is set by the plant characteristics.

Following [14], it is also of interest to study the sensitivity of (10) to structured uncertainty in the system matrix of the plant, and how it is influenced by the choice of Λ and τ.

Finally, the observer gain K has to be selected. This will mainly affect the state estimates behaviour in between impulses, and could be chosen e.g. as in a (steady-state) Kalman filter.

4 Numerical Example

In this section, the proposed technique for state estimation is validated on a numerical example, both with and without measurement noise. The observer

is applied to sampled data, with fast sampling (0.01 time units between each sample), to imitate continuous execution.

Assume the following values in (1)-(3)

$$A = \begin{bmatrix} -0.08 & 0 & 0 \\ 2 & -0.15 & 0 \\ 0 & 0.5 & -0.2 \end{bmatrix}, \qquad B = \begin{bmatrix} 1 \\ 0 \\ 0 \end{bmatrix}$$

$$C = \begin{bmatrix} 0 & 0 & 1 \end{bmatrix}, \qquad x_o = \begin{bmatrix} 4 \\ 20 \\ 60 \end{bmatrix}$$

with four impacting impulses

$$t_1 = 10 \qquad t_2 = 40, \qquad t_3 = 80 \qquad t_4 = 140$$
$$g_1 = 4 \qquad g_2 = 5 \qquad g_3 = 7 \qquad g_4 = 6.$$

To see the effect of measurement noise, white noise of zero mean and variance 10 was added to the output. The output $y(t)$ of the system is shown in Fig. 1. For the observer, the gain was chosen as

$$K = \begin{bmatrix} 0.0002 \\ 0.0048 \\ 0.0200 \end{bmatrix},$$

so that the eigenvalues of D are placed at $-0.1, -0.15$ and -0.2. The length of the sliding window was set to $\tau = 20$. Finally, Λ was chosen as

$$\Lambda = \{-2.65, -2.70, -2.75, -2.80, -2.85, -2.90\}.$$

For this set of parameters, it holds that

$$|E_i(\hat{t} - t_o)| < 10^{-7} |V_i(t_o + \tau - \hat{t})B|,$$

when $\hat{t} - t_o \leq 15$, cf. Proposition 3.2.

Thus, if the optimization problem in (18) is only solved when $\mathcal{T} \cap [t_o + 15, t_o + 20) = \emptyset$, then (19) is a good approximation.

Next a condition for adding an observer impulse should be chosen. In light of the discussion in Section 3.3, first consider $\|V(t_o + \tau - t_k)B\|$, which quantity is plotted in Fig. 2. The maximum in Fig. 2 occurs when $t_k - t_o \approx 5.8$, i.e. well below 15. This suggests choosing the optimization instants t_o in the observer such that the quantity $\|R(t)\|$ is at, or near, a maximum. Also, with this condition, the chosen optimization instants will not depend on the impulse weights. Hence, in this example, Step 1 of the algorithm in Section 3.1 will continue until $\|R(t)\|$ reaches a maximum.

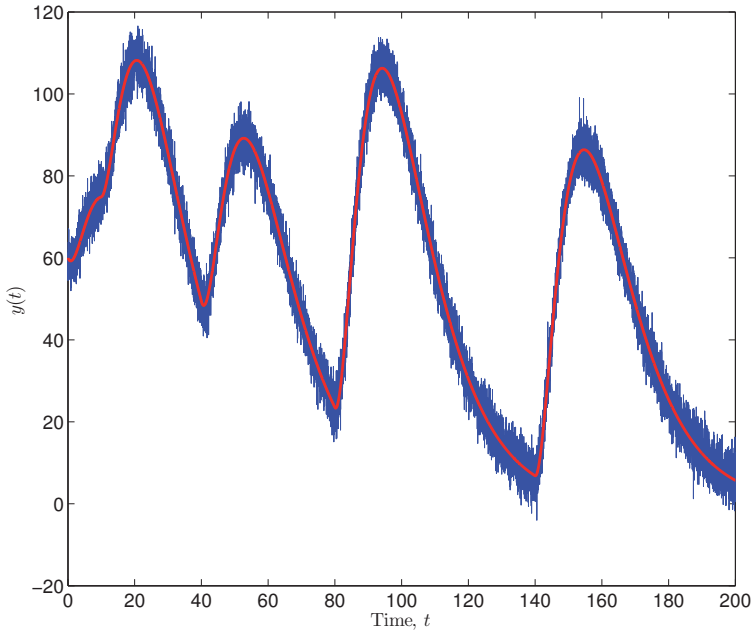

Figure 1: The output signal of the plant, with noise (blue line) and without (red line).

First the noise-free output was tested. In Fig. 3, the state estimates produced by the observer initialized with

$$\hat{x}(0) = \begin{bmatrix} 7 \\ 30 \\ 70 \end{bmatrix}$$

are shown together with true values of the plant states. The state estimation error $x(t) - \hat{x}(t)$, together with the quantity $e^{Dt}(x(0) - \hat{x}(0))$ are provided in Fig. 4. The latter characterizes the state estimation error that the observer would have with all observer impulses being identical to the plant impulses.

It can be seen that the proposed observer is completely off on the first impulse, but yet converges to the true state vector faster than it would if the first impulse were identical to the true plant impulse.

The observer was also tested with white measurement noise of variance 10 added to the output, see Fig. 1. The resulting state estimation error is presented in Fig. 5. Obviously, the estimated impulses are quite far from the true ones because of the measurement noise. In Section 3.6 it is seen that one way to reduce the sensitivity to noise is to move the elements of Λ

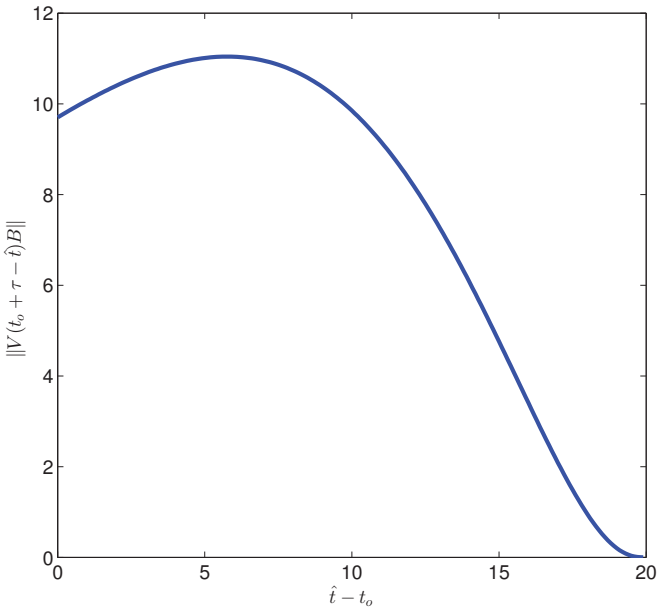

Figure 2: $\|V(t_o + \tau - t_k)B\|$ for $0 < t_k - t_o < \tau$.

closer to the origin. Therefore, the observer was also tested with

$$\Lambda = \{-0.65, -0.70, -0.75, -0.80, -0.85, -0.90\}$$

and the rest of the parameters left unchanged. The result for these parameters, with the noisy measurements of the output, is shown in Fig. 6. Clearly, the estimated impulses are much closer to the actual impulses in this case.

5 Conclusion

An observer for state estimation in linear time-invariant systems with unknown input impulses is suggested. The core of the method is to use a standard linear observer coupled with a state estimation algorithm employing finite-memory convolution operators. A numerical example demonstrates the feasibility of the proposed observer.

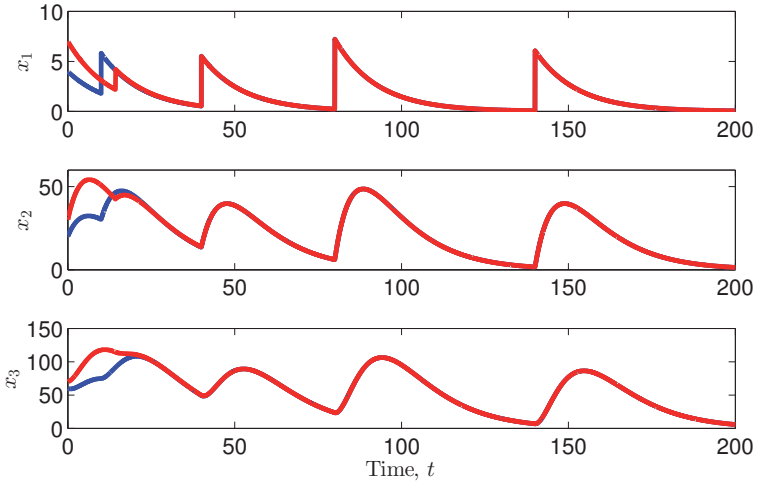

Figure 3: True states $x(t)$ (blue line), and estimated states $\hat{x}(t)$ (red line).

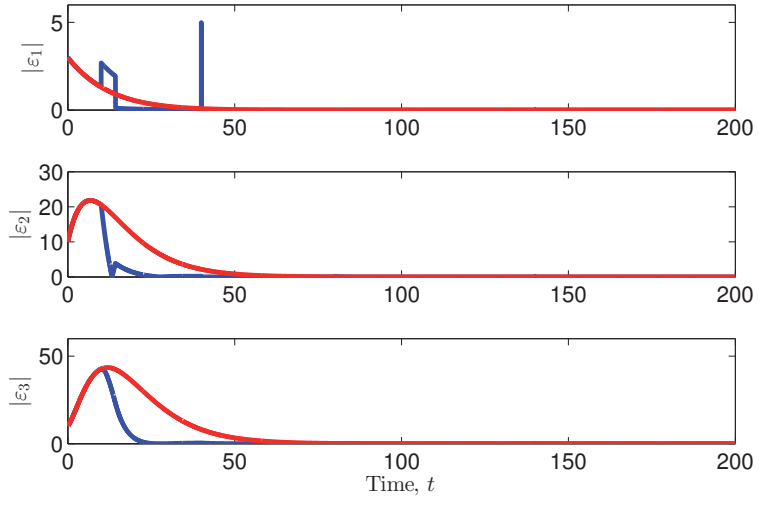

Figure 4: State estimation error $|x(t) - \hat{x}(t)|$ (blue line), and the state estimation error for an observer with exact knowledge of the plant impulses (red line).

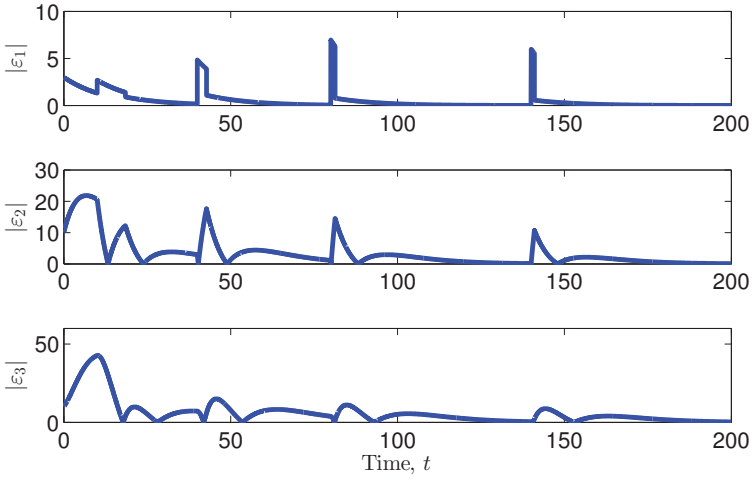

Figure 5: State estimation error $|x(t) - \hat{x}(t)|$, with original Λ, when measurement noise is added to the output.

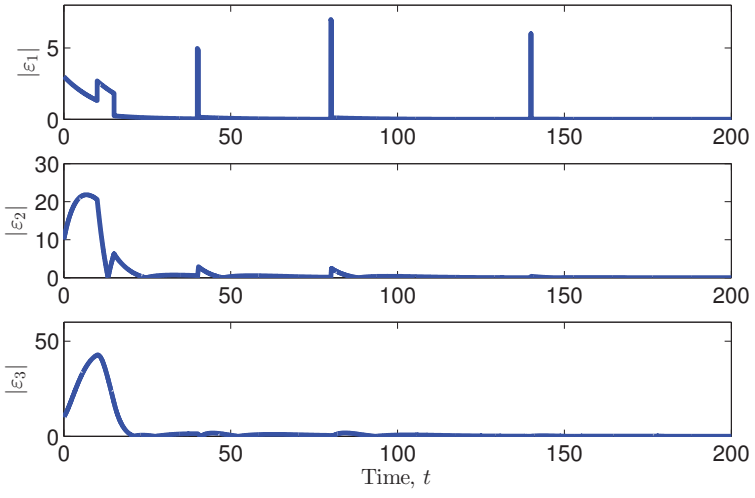

Figure 6: State estimation error $|x(t) - \hat{x}(t)|$, with modified Λ, when measurement noise is added to the output.

References

[1] W. Haddad, V. Chellaboina, and S. Nersesov, *Impulsive and Hybrid Dynamical Systems: Stability, Dissipativity, and Control*, ser. Princeton Series in Applied Mathematics. Princeton University Press, 2006.

[2] W. S. Evans, L. S. Farhy, and M. L. Johnson, "Biomathematical modeling of pulsatile hormone secretion: a historical perspective," in *Methods in Enzymology: Computer methods, Volume A*, M. L. Johnson and L. Brand, Eds., 2009, vol. 454, pp. 345–366.

[3] A. Churilov, A. Medvedev, and A. Shepeljavyi, "Mathematical model of non-basal testosterone regulation in the male by pulse modulated feedback," *Automatica*, vol. 45, no. 1, pp. 78–85, 2009.

[4] D. Luenberger, "Observers for multivariable systems," *IEEE Transactions on Automatic Control*, vol. 11, no. 2, pp. 190–197, apr 1966.

[5] Y. Tian, T. Floquet, L. Belkoura, and W. Perruquetti, "Algebraic switching time identification for a class of linear hybrid systems," *Nonlinear Analysis: Hybrid Systems*, vol. 5, no. 2, pp. 233 – 241, 2011.

[6] T. Raff and F. Allgower, "An impulsive observer that estimates the exact state of a linear continuous-time system in predetermined finite time," in *Mediterranean Conference on Control Automation*, june 2007, pp. 1–3.

[7] G. Zheng, Y. Orlov, W. Perruquetti, and J.-P. Richard, "Finite-time observer-based control of linear impulsive systems with persistently acting impact," in *IFAC World Congress*, Milano, Italy, Aug. 2011.

[8] E. Medina and D. Lawrence, "State estimation for linear impulsive systems," in *American Control Conference*, june 2009, pp. 1183–1188.

[9] A. Churilov, A. Medvedev, and A. Shepeljavyi, "A state observer for continuous oscillating systems under intrinsic pulse-modulated feedback," *Automatica*, vol. 48, no. 6, pp. 1117–1122, 2012.

[10] ——, "Further results on a state observer for continuous oscillating systems under intrinsic pulsatile feedback," in *50th IEEE Conference on Decision and Control and European Control Conference (CDC-ECC)* , dec. 2011, pp. 5443–5448.

[11] P. Mattsson and A. Medvedev, "Estimation of input impulses by means of continuous finite memory observers," in *American Control Conference*, june 2012, pp. 6769–6774.

[12] A. Medvedev, "Continuous least-squares observers with applications," *IEEE Transactions on Automatic Control*, vol. 41, no. 10, pp. 1530–1537, oct 1996.

[13] ——, "Disturbance attenuation in finite-spectrum-assignment controllers," *Automatica*, vol. 33, no. 6, pp. 1163–1168, 1997.

[14] A. Medvedev and H. T. Toivonen, "Directional sensitivity of continuous least-squares state estimators." *Systems & Control Letters*, vol. 59, no. 9, pp. 571–577, 2010.

A Proof of Proposition 3.2

The relation in (14) follows from the fact that

$$\varepsilon(t_o+\tau) = e^{D\tau}\varepsilon(t_o) + g_k e^{D(t_o+\tau-t_k)}B - \hat{g}_l e^{D(t_o+\tau-\hat{t}_l)}B.$$

To prove the last part of the proposition assume, without loss of generality, that $t_o = 0$.

Let $C_i = C(\lambda_i I - D)^{-1}$. The rows of $E(\hat{t})$ are given by

$$E_i(\hat{t}) = C_i\left(e^{(\lambda_i I-D)\tau} - e^{(\lambda_i I-D)(\tau-\hat{t})}\right)e^{D(\tau-\hat{t})}B = e^{\lambda_i(\tau-\hat{t})}C_i\left(e^{(\lambda_i I-D)\hat{t}} - I\right)B.$$

Notice that, for fixed $\hat{t} > 0$,

$$\left|C_i(e^{(\lambda_i I-D)\hat{t}} - I)B\right| \to 0, \text{ as } \lambda_i \to -\infty.$$

Similarily, the rows of $V(\tau-\hat{t})B$ are found to be

$$V_i(\hat{t})B = C_i\left(e^{(\lambda_i I-D)(\tau-\hat{t})} - I\right)e^{D(\tau-\hat{t})}B = -e^{\lambda_i(\tau-\hat{t})}C_i\left(e^{(D-\lambda_i I)(\tau-\hat{t})} - I\right)B.$$

Note that, for fixed $0 < \hat{t} < \tau$,

$$\left|C_i(e^{(D-\lambda_i I)(\tau-\hat{t})} - I)B\right| \to \infty, \text{ as } \lambda_i \to -\infty.$$

Hence, it can be concluded that, for $0 < \hat{t} < \tau$,

$$\frac{|E_i(\hat{t})|}{|V_i(\hat{t})B|} = \frac{|C_i(e^{(\lambda_i I-D)\hat{t}} - I)B|}{|C_i(e^{(D-\lambda_i I)(\tau-\hat{t})} - I)B|} \to 0, \text{ as } \lambda_i \to -\infty$$

and thus the result of the proposition follows.

Paper III

Periodical Solutions in a Pulse-modulated Model of Endocrine Regulation with Time-delay

Alexander Churilov, Alexander Medvedev, and Per Mattsson[‡]

Abstract

A hybrid mathematical model of endocrine regulation obtained by augmenting the classical continuous Smith model with a pulse-modulated feedback to describe episodic (pulsatile) secretion is considered. Conditions for existence and local orbital stability of periodical solutions with m impulses in the least period (m-cycles) are derived. An important implication of the performed analysis is that the nonlinear dynamics of the pulse-modulated system and not the delay itself cause the sustained closed-loop oscillations. Furthermore, simulation and bifurcation analysis indicate that increasing the time delay in the system in hand typically, but not always, leads to less complex dynamic pattern in the closed-loop system by giving rise to stable cycles of lower periodicity.

1 Introduction

Hormones are the signaling substances of endocrine systems that regulate many aspects in the human body, i.e. metabolism, growth as well as the sexual function and the reproductive processes. Hormones are secreted by endocrine glands directly into the bloodstream in continuous (basal) or pulsatile (non-basal) manner. Endocrine glands, interacting via hormone concentrations in blood, build up dynamical control loops characterized by self-sustained oscillations of the involved physiological quantities, [1].

Oscillations in biological feedback systems arise for a broad range of system parameters which property is not always captured by the mathematical models, [2]. With respect to mathematical models of endocrine regulation,

[*]A. Medvedev and P. Mattsson were in part financed by the European Research Council, Advanced Grant 247035 (SysTEAM).

[†]A. Churilov is with the Department of Mathematics and Mechanics, St. Petersburg State University, St. Petersburg, Russia.

[‡]A. Medvedev and P. Mattsson are with Information Technology, Uppsala University, Uppsala, Sweden.

mostly nonlinear feedback and time delays were employed for achieving sustained periodical solutions. The Smith model of testosterone regulation [3] is proven to be asymptotically stable for any value of the time delay and the nonlinear feedback in the form of a first-order Hill function, [4]. However, under piecewise linear (affine) feedback nonlinearities, multiple periodical orbits and chaos arise in the Smith model [5, 6]. Multiple delays in the Smith model under a second-order Hill function feedback are also shown to lead to sustained nonlinear oscillations in some subspaces of the model parameters [7]. Naturally, the equilibrium point of the model dynamics has to be rendered unstable.

The concept of amplitude and frequency pulse-modulated feedback appears naturally in non-basal hormone regulation and is widely accepted. The rationale is given e.g. in [8]. A hybrid parsimonious mathematical model describing pulsatile endocrine regulation and lending itself to mathematical analysis is suggested in [9] and studied in detail in [10]. The model does not, by design, have any equilibria and always possesses a 1-cycle, i.e. a periodic solution with one pulse in the least period. It is also shown to exhibit complex nonlinear dynamics such as cycles of higher periodicity and chaos [11]. The latter discovery confirms that the pulse-modulated model in question is able to produce signaling patterns of any dynamical complexity. However, in its original formulation, the pulse-modulated model of hormone secretion does not take into account the presence of a time delay in the closed loop that is a significant phenomenon in many endocrine systems. Time delay is present in endocrine systems mainly due to two circumstances. First, there is a delay due to the transport of the hormones in the blood stream. Second, a delay also results from the lack of releasable pools of the hormone and the need to synthesize it before secretion [8].

With the time delay taken into account, the pulse-modulated model of endocrine regulation acquires an infinite-dimensional continuous part. The closed-loop dynamics are therefore both hybrid and infinite dimensional, which combination is mathematically challenging and so far rarely treated. The existing theory of impulsive delay-differential equations (see, e.g., [12, 13]) does not readily provide the tools for an exhaustive analysis of the model under consideration. The present study is therefore aimed to fill the existing gap in mathematical modeling of non-basal endocrine feedback regulation and provide insights into the dynamical phenomena occurring in pulse-modulated models of such systems due to the time delay.

In this paper, existence and stability conditions for periodical solutions in a time-delay pulse-modulated model of non-basal endocrine regulation are derived in a general mathematical framework and specialized to the case of testosterone regulation in the human male. The paper is organized as follows. First a brief background on linear time-delay systems is provided

and the notion of finite-dimension reducible system is introduced. Then a (hybrid) model describing a continuous time-delay system controlled by a pulse-modulated feedback is formulated, followed, under the assumption of finite-dimensional reducibility, by a detailed analysis of existence and stability of the closed-loop behaviors. Finally, the obtained theoretical results are applied to the case of non-basal testosterone regulation in the male and validated through simulation and numerical calculations.

2 Finite-Dimension Reducible Linear Time Delay Systems

Consider an autonomous time-delay system

$$\frac{dx}{dt} = A_0 x(t) + A_1 x(t-\tau), \tag{1}$$

where $x(t) \in \mathbb{R}^p$ is the state vector, $A_0, A_1 \in \mathbb{R}^{p\times p}$ are square constant matrices, $A_1 \neq 0$, and $\tau \neq 0$ is a constant time delay. System (1) is subject to the initial conditions $x(t) = \varphi(t)$, $-\tau \leqslant t \leqslant 0$, where $\varphi(t)$ is a continuous vector function.

The following property of time-delay systems is of principal importance for the exposition.

Definition 1. *Time-delay linear system* (1) *is called* finite-dimension reducible (FD-reducible) *if*

$$A_1 A_0^k A_1 = 0 \quad \textit{for all} \quad k = 0, 1, \ldots, p-1. \tag{2}$$

The property of FD-reducibility is not particularly liming when it comes to endocrine systems. Indeed, a simple endocrine axis typically constitutes a cascade coupling of non-oscillatory blocks representing the concentrations of individual hormones with time delays in between. In such a system, FD-reducibility is equivalent to the lack of local feedback around the time-delay block.

Obviously, relationships (2) can be equivalently rewritten as

$$A_1 \mathrm{e}^{A_0 t} A_1 = 0 \quad \text{for all} \quad t \geqslant 0. \tag{3}$$

Lemma 1. *System* (1) *is FD-reducible iff there exists an invertible* $p \times p$ *matrix* S *such that*

$$S^{-1} A_0 S = \begin{bmatrix} U & 0 \\ W & V \end{bmatrix}, \quad S^{-1} A_1 S = \begin{bmatrix} 0 & 0 \\ \bar{W} & 0 \end{bmatrix}, \tag{4}$$

where the blocks U, V *are square, the sizes of the blocks* W *and* $\bar{W}$ *are equal, and the matrix pair* $(\bar{W}, U)$ *is observable (see, e.g., [14]).*

The theorem can be proved by state space transformation, [14]. The block structure of the matrices in (4) clearly relates to the models of endocrine systems with time delay between the compartments and is often encountered in endocrine axes with feedback non-basal regulation, see e.g. [15]. Under the assumption of FD-reducibility, system (1) posesses a cascade (feedforward) structure comprising finite-dimensional blocks revealed by the block-triangular structure of the transformed matrix A_0 in (4) and interconnected by a pure time delay, as implied by the nilpotent A_1.

Corollary 1. *Let system* (1) *be FD-reducible. Then for any complex* s *and any real* τ *one has*

$$\det(A_0 + A_1 \mathrm{e}^{-\tau s} - sI_p) = \det(A_0 - sI_p).$$

The result follows from the block structure specified in (4). Thus the spectrum of an FD-reducible system (1) is finite and independent of the delay τ. Time-delay systems with finite spectrum appear e.g. in the classical control problem of finite spectrum assignment, see [16, 17].

Introduce the matrix $D = A_0 + A_1 \mathrm{e}^{-A_0 \tau}$. Following [18], consider a fundamental solution of (1), namely a function $X(t, t_0)$ with the properties: $X(t, t_0) = 0$ for $t < t_0$, $X(t_0, t_0) = I_p$, and

$$\frac{\partial X}{\partial t} = A_0 X(t, t_0) + A_1 X(t - \tau, t_0) \quad \text{for} \quad t \geqslant t_0. \tag{5}$$

Theorem 1. *Let system* (1) *be FD-reducible. Then* $X(t, t_0) = H(t - t_0)\Psi(t - t_0)$*, where*

$$\Psi(t) = \begin{cases} \mathrm{e}^{A_0 t}, & t \leqslant \tau, \\ \mathrm{e}^{D(t-\tau)} \mathrm{e}^{A_0 \tau}, & t \geqslant \tau, \end{cases} \tag{6}$$

and $H(t)$ *is the Heaviside step function. (Here* $H(0) = 1$*.)*

Proof. From the block representation in (4), any solution $x(t)$ of (1) satisfies the linear differential equation

$$\frac{dx}{dt} = Dx \tag{7}$$

for $t \geqslant \tau$. Then (6) follows immediately. □

It is seen from (7) that time-delay system (1) behaves as a finite-dimensional system of dimension p on the time interval $[\tau, +\infty)$ while its infinite-dimensional nature is revealed only on the segment $[0, \tau]$.

Lemma 2. *The following relationships are true:*

$$A_1 \Psi(t) = A_1 \mathrm{e}^{A_0 t}, \quad \Psi(t) A_1 = \mathrm{e}^{A_0 t} A_1 \quad \textit{for all} \quad t. \tag{8}$$

Proof. Lemma 2 is a straightforward consequence of Theorem 1 and Lemma 1 and follows from the block representation (4). □

Introduce, for further use, the matrix functions

$$\Psi_0(t) = H(t-\tau)\mathrm{e}^{A_0(t-\tau)}$$

and

$$\begin{aligned} Q(t,\xi) &= \int_{-\tau}^{0} \Psi_0(t-\theta)A_1\mathrm{e}^{A_0(\theta+\xi)}\,d\theta, \\ Q_0(t,\xi) &= \mathrm{e}^{A_0(t-\tau)}\left(\mathrm{e}^{D\tau} - \mathrm{e}^{A_0\tau}\right)\mathrm{e}^{A_0\xi}. \end{aligned} \tag{9}$$

Lemma 3. *The following relationship holds:*

$$Q(t,\xi) = \begin{cases} \left(\mathrm{e}^{Dt} - \mathrm{e}^{A_0 t}\right)\mathrm{e}^{A_0\xi}, & t \leqslant \tau, \\ Q_0(t,\xi), & t \geqslant \tau. \end{cases}$$

Proof. By using the block form (4) of the matrices A_0, A_1 it can be shown that if system (1) is FD-reducible, then

$$\int_{t_0}^{t} \mathrm{e}^{A_0(t-\theta)}A_1\mathrm{e}^{A_0(\theta-t_0)}d\theta = \left(\mathrm{e}^{D(t-t_0)} - \mathrm{e}^{A_0(t-t_0)}\right)\mathrm{e}^{A_0\tau} \tag{10}$$

for any real t, t_0. Clearly, the matrix function $Q(t,\xi)$ can be written as

$$Q(t,\xi) = \int_{-\tau}^{\min\{t-\tau,0\}} \mathrm{e}^{A_0(t-\tau-\theta)}A_1\mathrm{e}^{A_0(\theta+\xi)}\,d\theta.$$

Now Lemma 3 follows from (10). □

From (3), (9) and Lemma 3, it is seen that

$$A_1Q(t,\xi) = A_1Q_0(t,\xi) \equiv 0 \quad \text{for all} \quad t,\ \xi. \tag{11}$$

Lemma 4. *Let $x(t)$ be a solution of an FD-reducible system* (1) *and $t_0 \geqslant 0$. Then*

$$x(t) = \Psi(t-t_0)x(t_0) + \int_{-\tau}^{0} \Psi_0(t-t_0-\theta)A_1x(\theta+t_0)\,d\theta \tag{12}$$

for $t \geqslant t_0$.

Proof. From [18] one has

$$x(t) = X(t,t_0)x(t_0) + \int_{t_0-\tau}^{t_0} X(t,\theta+\tau)A_1x(\theta)\,d\theta \tag{13}$$

for $t \geqslant t_0$. From Theorem 1, it follows that

$$x(t) = \Psi(t-t_0)x(t_0) + \int_{t_0-\tau}^{t_0} H(t-\tau-\theta)\Psi(t-\tau-\theta)A_1 x(\theta)\,d\theta \qquad (14)$$

for $t \geqslant t_0$. Then (14) and the second equality in (8) imply the sought result of the lemma. □

Next, an alternative description of the evolution operator generated by (1) is provided.

Lemma 5. *Let $x(t)$ be a solution of an FD-reducible system* (1)*. Pick two numbers t_0, t_1 satisfying $t_0 \geqslant 0$ and $t_1 - t_0 \geqslant \tau$. Then, it holds that*

$$x(t) = \Psi(t-t_1)x(t_1) + Q(t-t_1, t_1-t_0)x(t_0) \qquad (15)$$

for $t \geqslant t_1$.

Proof. It follows from (12) that

$$A_1 x(t) = A_1\Psi(t-t_0)x(t_0) \quad \text{for} \quad t \geqslant t_0.$$

Due to Lemma 4

$$x(t) = \Psi(t-t_1)x(t_1) + \int_{-\tau}^{0} \Psi_0(t-t_1-\theta)A_1 x(\theta+t_1)\,d\theta, \qquad (16)$$

for $t \geqslant t_1$. Hence, for $t_1 - \tau \geqslant t_0$, (16) can be rewritten as

$$x(t) = \Psi(t-t_1)x(t_1) + \int_{-\tau}^{0} \Psi_0(t-t_1-\theta)A_1\Psi(\theta+t_1-t_0)\,d\theta\; x(t_0).$$

Then Lemma 5 follows from (9). □

The relationship (15) shows that a solution $x(t)$ satisfying (1) for $t \geqslant t_1$ is completely defined by two initial finite-dimensional vectors, i.e. $x(t_0)$ and $x(t_1)$. This property is in contrast with general time-delay systems of type (1) and explains the name of the above introduced notion of FD-reducibility.

3 A Time-Delay Impulsive System

Consider an extension of the impulsive model of non-basal endocrine regulation treated iN [9, 10] to the class of systems with delayed continuous part:

$$\begin{aligned} \frac{dx}{dt} &= A_0 x(t) + A_1 x(t-\tau), \qquad y = Cx, \\ t_{n+1} &= t_n + T_n, \qquad x(t_n^+) = x(t_n^-) + \lambda_n B, \\ T_n &= \Phi(y(t_n)), \qquad \lambda_n = F(y(t_n)). \end{aligned} \qquad (17)$$

where B is a vector and C is a row such that $CB = 0$. Thus, the signal that is fed back through the pulse-modulated feedback is scalar. The relationship between C and B safeguards the continuity of the output y. Without loss of generality assume $t_0 = 0$. For brevity sake denote $\bar{x}_n = x(t_n^-)$.

Model (17) is effectively a so-called Smith model [19] with a pulse-modulated feedback.

The continuous functions $\Phi(\cdot)$, $F(\cdot)$, representing respectively frequency and amplitude modulation [20], satisfy

$$0 < \Phi_1 \leqslant \Phi(\cdot) \leqslant \Phi_2, \qquad 0 < F_1 \leqslant F(\cdot) \leqslant F_2, \tag{18}$$

for some constants $\Phi_i, F_i, i = 1, 2$. The latter condition implies that system (9) has no equilibria and thus eliminates the main shortcoming of the classical Smith model, see [4]. In the context of endocrine system, the function $\Phi(\cdot)$ defines the time instants when hormone pulses are fired while $F(\cdot)$ is used to evaluate their magnitudes.

Since the linear part of the system represents the kinetics of the involved hormones, it has to be stable, i.e., all the roots of the characteristic equation $\det(sI_p - A_0 - A_1 \mathrm{e}^{-\tau s}) = 0$ have to satisfy $\operatorname{Re} s < 0$. Furthermore, the continuous part of system (17) is henceforth assumed to be FD-reducible. Then, as it follows from Corollary 1 to Lemma 1, stability of the linear part of (17) is ensured by Hurwitz stability of the matrix A_0.

Besides of stability of the continuous part of the model under consideration, it is also biologically feasible that all the solutions of (17) are bounded. The bondedness of all the solutions for $t \geqslant 0$ follows from inequality (18) and from the FD-reducibility (namely, from representation (4)).

Lemma 6. *Assume that*

$$\inf_y \Phi(y) > \tau \tag{19}$$

and the initial function $\varphi(t)$, $-\tau \leqslant t \leqslant 0$ is continuous. Then (17) is satisfied by $x(t)$ defined as follows.

For $0 < t < t_1$,

$$x(t) = \Psi(t)(\bar{x}_0 + \lambda_0 B) + \int_{-\tau}^{0} \Psi_0(t - \theta) A_1 \varphi(\theta)\, d\theta. \tag{20}$$

For $n \geqslant 1$ and $t_n < t < t_{n+1}$,

$$x(t) = \Psi(t - t_n)(\bar{x}_n + \lambda_n B) + Q(t - t_n, T_{n-1})(\bar{x}_{n-1} + \lambda_{n-1} B), \tag{21}$$

where the function $Q(t, \xi)$ is given by (9).

Proof. From Lemma 4 for $t_n < t < t_{n+1}$, $n \geqslant 0$

$$x(t) = \Psi(t - t_n)x(t_n^+) + \int_{-\tau}^{0} \Psi_0(t - t_n - \theta)A_1 x(\theta + t_n)\, d\theta. \tag{22}$$

Since $t_0 = 0$, (22) implies (20) for $n = 0$.

From (3), (8) and (22) it is concluded that

$$A_1 x(t) = A_1 \mathrm{e}^{A_0(t-t_n)}(\bar{x}_n + \lambda_n B), \quad t_n < t < t_{n+1}. \tag{23}$$

Consider $n \geqslant 1$. Then from (19) $t_{n-1} < t_n - \tau \leqslant t_n + \theta \leqslant t_n$ as $-\tau \leqslant \theta \leqslant 0$. Hence from (23)

$$A_1 x(t_n + \theta) = A_1 \mathrm{e}^{A_0(t_n+\theta-t_{n-1})}(\bar{x}_{n-1} + \lambda_{n-1} B) \tag{24}$$

for $-\tau \leqslant \theta \leqslant 0$. Substitute (24) into (22) to obtain (21). □

4 A Discrete-Time System

In this section, it is demonstrated that impulsive system (17) with an FD-reducible continuous part can be described by discrete dynamics at the instants t_n, $n = 0, 1, \ldots$.

Define a matrix function $P(x, z)$ that maps p-dimensional vectors x and z into a p-dimensional vector

$$\begin{aligned} P(x, z) = {} & \Psi(\Phi(Cx))[x + F(Cx)B] \\ & + Q_0(\Phi(Cx), \Phi(Cz))[z + F(Cz)B], \end{aligned} \tag{25}$$

where $Q_0(t, \xi)$ is given by (9). Consider a sequence of vectors $\bar{x}_n = x(t_n^-)$. Introduce also

$$T_n = \Phi(C\bar{x}_n), \quad \lambda_n = F(C\bar{x}_n), \quad n = 0, 1, \ldots.$$

In particular,

$$T_0 = \Phi(C\varphi(0)), \quad \lambda_0 = F(C\varphi(0)),$$

where $\varphi(t)$ is the initial function of (17).

Lemma 7. *Let* (19) *be satisfied and* $\varphi(t)$, $-\tau \leqslant t \leqslant 0$ *be a continuous initial function. Then the vectors* x_n *satisfy the recursion*

$$\bar{x}_{n+1} = P(\bar{x}_n, \bar{x}_{n-1}), \qquad n \geqslant 1, \tag{26}$$

with the initial values $\bar{x}_0 = \varphi(0)$,

$$\bar{x}_1 = \Psi(T_0)(\bar{x}_0 + \lambda_0 B) + \mathrm{e}^{A_0(T_0-\tau)} \int_{-\tau}^{0} \mathrm{e}^{-A_0\theta} A_1 \varphi(\theta)\, d\theta. \tag{27}$$

Proof. Equations (27), (26) are obtained by setting $t = t_1$ in (20) and $t = t_{n+1}$ in (21), respectively. Since by (19) $t_{n+1} - t_n > \tau$, due to Lemma 3, Q_0 can be substituted by Q. □

For discrete time dynamical system (26), the sequence $\bar{x}_0,\ \bar{x}_1,\ \bar{x}_2, \ldots$, can be termed as the forward orbit of the initial point $(\bar{x}_0, \bar{x}_1)$.

Notice that, contrary to the delay-free case considered in [10], the knowledge of the sequence $\bar{x}_n$ is not sufficient to reconstruct the inter-impulse behavior of the continuous time system solution $x(t)$. Indeed, in general, the initial function $\varphi(t)$ cannot be uniquely found from integral equation (27). However, it will be shown in the next section that such reconstruction becomes possible provided $x(t)$ is periodic.

5 Existence of Cycles

The existence conditions for periodic solutions with m impulses in the least period (m-cycles) of pulse-modulated time delay system (17) are investigated in this section. Evidently, every such solution gives rise to an m-periodic forward orbit of discrete map (26). It will be shown below that the converse statement is also true: every m-periodic orbit corresponds to a unique initial function for a solution with m impulses in the least period.

Let the matrix functions $Q(t, \xi)$, $Q_0(t, \xi)$ be as in (9).

Theorem 2 (existence of a 1-cycle)**.** *Let* (19) *be satisfied. Suppose that there exists a vector* $\bar{x}_0$ *such that*

$$\bar{x}_0 = [\Psi(T_0) + Q_0(T_0, T_0)]\,(\bar{x}_0 + \lambda_0 B), \tag{28}$$

where $T_0 = \Phi(C\bar{x}_0)$, $\lambda_0 = F(C\bar{x}_0)$. *Then there exists a* T_0*-periodic 1-cycle with the initial function defined by*

$$\varphi(t) = [\Psi(t + T_0) + Q(t + T_0, T_0)]\,(\bar{x}_0 + \lambda_0 B), \quad -\tau \leqslant t \leqslant 0. \tag{29}$$

Conversely, if there exists a 1-cycle then the vector $\bar{x}_0 = \varphi(0)$ *satisfies* (28) *with the initial function* $\varphi(t)$ *given by* (29).

Proof. To obtain a 1-cycle it suffices to ensure that

$$x(t + T_0) = \varphi(t), \quad -\tau \leqslant t < 0.$$

By means of (20) this can be rewritten for $-\tau \leqslant t < 0$ as

$$\varphi(t) = \Psi(t + T_0)(\bar{x}_0 + \lambda_0 B) + \int_{-\tau}^{0} \Psi_0(t + T_0 - \theta) A_1 \varphi(\theta)\, d\theta\,. \tag{30}$$

Multiply (30) by A_1 from the left. Then

$$A_1\varphi(t) = A_1\Psi(t+T_0)(\bar{x}_0 + \lambda_0 B) = A_1 \mathrm{e}^{A_0(t+T_0)}(\bar{x}_0 + \lambda_0 B)$$

for $-\tau \leqslant t < 0$. Substitute the last equality into (30) to get

$$\varphi(t) = \left[\Psi(t+T_0) + \int_{-\tau}^{0} \Psi_0(t+T_0-\theta) A_1 \mathrm{e}^{A_0(\theta+T_0)}\, d\theta\right] \times (\bar{x}_0 + \lambda_0 B), \quad -\tau \leqslant t < 0,$$

which yields (29). Setting $t = 0$ in (29) and employing (28) gives $\varphi(0) = \bar{x}_0$. □

Theorem 3 (existence of an m-cycle)**.** *Let* (19) *be satisfied. Consider an integer number $m \geqslant 2$. Suppose that there exist vectors $\bar{x}_0, \ldots, \bar{x}_{m-1}$ such that $\bar{x}_i \neq \bar{x}_j$ for $i \neq j$ and*

$$\begin{aligned} \bar{x}_0 &= P(\bar{x}_{m-1}, \bar{x}_{m-2}), \\ \bar{x}_1 &= P(\bar{x}_0, \bar{x}_{m-1}), \\ \bar{x}_n &= P(\bar{x}_{n-1}, \bar{x}_{n-2}), \quad n = 2, \ldots, m-1 \quad (\textit{for} \quad m \geqslant 3). \end{aligned} \tag{31}$$

Let $T_n = \Phi(C\bar{x}_n)$, $\lambda_n = F(C\bar{x}_n)$, $n = 0, 1, \ldots, m-1$. Then there exists an m-cycle with the period

$$T = T_0 + \ldots + T_{m-1},$$

and the initial function defined on the interval $-\tau \leqslant t \leqslant 0$ by

$$\begin{aligned} \varphi(t) = {} & \Psi(t+T_{m-1})(\bar{x}_{m-1} + \lambda_{m-1}B) \\ & + Q(t+T_{m-1}, T_{m-2})(\bar{x}_{m-2} + \lambda_{m-2}B). \end{aligned} \tag{32}$$

Conversely, if there exists an m-cycle then the vectors $\bar{x}_n = x(t_n^-)$, $n = 0, \ldots, m-1$, are all distinct and satisfy (31)*, and the initial function $\varphi(t)$ is determined by* (30)*.*

Proof. For an m-cycle, one has to ensure

$$x(t+T) = \varphi(t), \quad -\tau \leqslant t < 0. \tag{33}$$

It is easily seen that

$$T = t_1 + (t_2 - t_1) + \ldots + (t_m - t_{m-1}) = t_m.$$

Since $T_{m-1} = t_m - t_{m-1} > \tau$ and $t + T = t + t_m$, $t_{m-1} < t + T < t_m$ as $-\tau \leqslant t < 0$. Using (21), rewrite (33) for $-\tau \leqslant t < 0$ as

$$\begin{aligned} \varphi(t) = {} & \Psi(t+T-t_{m-1})(\bar{x}_{m-1} + \lambda_{m-1}B) \\ & + Q(t+T-t_{m-1}, T_{m-2})(\bar{x}_{m-2} + \lambda_{m-2}B), \end{aligned} \tag{34}$$

where $T - t_{m-1} = t_m - t_{m-1} = T_{m-1}$, so (34) implies (32). Then the relationship $\varphi(0) = \bar{x}_0$ is equivalent to the first equality in (31).

From (32), (8) and (11), it follows that for $-\tau \leqslant t \leqslant 0$

$$A_1\varphi(t) = A_1 \mathrm{e}^{A_0(t+T_{m-1})}(\bar{x}_{m-1} + \lambda_{m-1}B).$$

By substituting the expression above into (27), one arrives to the second equality in (31). The rest of equalities in (31) are simply reformulations of the relationships in (26). The converse statement of the theorem is straightforward. □

In fact, condition (19) is often satisfied in endocrine systems, providing a hint to what can be considered as "small" time delays in the present context. Evidently, under these conditions the periodic dynamics of the time delay system are uniquely (including the inter-impulse behavior) defined by the discrete mapping of (26).

6 Stability of Cycles

Since system (17) has no equilibria, stability of its solutions is understood as stability of the corresponding orbit with respect to small perturbations in the initial data, paying special attention to periodic orbits.

For a solution $(x(t),\ t_n)$ of system (17) with a continuous initial function $\varphi(t)$, consider continuous perturbed functions $\tilde{\varphi}(t)$ that are close to $\varphi(t)$, namely such that the norm

$$\|\tilde{\varphi} - \varphi\|_\infty = \sup_{-\tau \leqslant t \leqslant 0} \|\tilde{\varphi}(t) - \varphi(t)\|$$

is small, where $\|\cdot\|$ is the Euclidean vector norm.

As previously, let $\bar{x}_n = x(t_n^-)$. A solution $x(t)$ will be called *stable* if for any $\varepsilon > 0$ there exists a number $\varepsilon_0 > 0$ such that for a perturbed solution $(\tilde{x}(t), \tilde{t}_n)$ with a continuous initial function $\tilde{\varphi}(t)$, $\tilde{t}_0 = 0$, and $\tilde{x}_n = \tilde{x}(\tilde{t}_n^-)$ such that $\|\tilde{\varphi}(t) - \varphi(t)\|_\infty < \varepsilon_0$, it applies that $\|\bar{x}_n - \tilde{x}_n\| < \varepsilon$ for all $n \geqslant 0$. A solution $x(t)$ will be called *asymptotically stable* if it is stable and, moreover, there exists a number $\varepsilon_1 > 0$ such that $\|\bar{x}_n - \tilde{x}_n\| \to 0$ as $n \to \infty$, provided that $\|\tilde{\varphi}(t) - \varphi(t)\|_\infty < \varepsilon_1$.

As it is seen from (27), when $\|\tilde{\varphi}(t) - \varphi(t)\|_\infty$ is small then $\tilde{x}_0$ and $\tilde{x}_1$ are close to $\bar{x}_0$ and $\bar{x}_1$, respectively. Thus, the consideration can be limited to local stability of forward orbits of discrete map (26).

Rewrite (26) in terms of a new variable $\bar{z}_n = \bar{x}_{n-1}$ for $n \geqslant 1$. Then (26) turns into a first order system

$$\bar{x}_{n+1} = P(\bar{x}_n, \bar{z}_n), \qquad \bar{z}_{n+1} = \bar{x}_n, \tag{35}$$

where $P(x,z)$ is defined by (25). Together with the initial conditions $\bar{x}_1$, $\bar{z}_1 = \bar{x}_0$, equations (35) completely characterize the dynamics of system (17). Let the functions $\Phi(y)$ and $F(y)$ have continuous derivatives. Then a Jacobian $J(\bar{x},\bar{z})$ of the map (35) can be easily obtained by a direct calculation and a local stability analysis is straightforward (see, e.g., [21]).

7 Time-Delay Impulsive Model of Testosterone Regulation

In this section, the theoretical tools developed above are applied to a delayed system with impulsive feedback that originates from modeling of the GnRH—LH—Te endocrine axis [3, 7, 19, 22–26].

In what follows, only the dominating delay from pituitary, where LH is secreted, to testes, where Te is produced, is considered. The delay value τ takes into account not only the transport of LH from pituitary to testes, but also an additional time required to stimulate steroid synthesis in the testes, [22]. There are other delays in this endocrine axis that also can be included in the model, but this would however unnecessary complicate the equations. The main goal of this section is to demonstrate how a time delay in the continuous part of the axis effects the nonlinear dynamics of the closed-loop endocrine system.

In [22], the following delays are suggested: from hypothalamus to pituitary — 3 min, from pituitary to testes — 5 min, from testis to hypothalamus — 5 min, the interval between testes stimulation and testosterone release — 25 min. So the total delay from secretion of LH to secretion of Te in the testes is $\tau = 5 + 25 = 30$ min. The delay τ is less than a half-period of the ultradian rhythm, with an average cycle of 1.9–2.3 hrs, and thus satisfies assumption (19). Therefore, the effective delay can be characterized as "small", in the closed-loop context of pulse-modulated systems, despite its seemingly significant value.

Consider a specialization of system (17) with

$$\begin{aligned}
\frac{dx_1}{dt} &= -b_1 x_1, \quad \frac{dx_2}{dt} = -b_2 x_2 + g_1 x_1,\\
\frac{dx_3}{dt} &= -b_3 x_3 + g_2 x_2(t-\tau),\\
t_0 &= 0, \quad t_{n+1} = t_n + T_n,\\
x_1(t_n^+) &= x_1(t_n^-) + \lambda_n,\\
T_n &= \Phi(x_3(t_n)), \quad \lambda_n = F(x_3(t_n)),
\end{aligned} \tag{36}$$

where $b_1 = 0.4$, $b_2 = 0.01$, $b_3 = 0.046$, $g_1 = 2$, $g_2 = 4$. The values for b_i, $i = 1, 2, 3$ correspond to the half-life time of GnRH, LH and Te, respectively, and are calculated according to the biochemical data for the hormones typically provided in the literature, see e.g. [24].

The modulation functions are selected as Hill functions

$$\Phi(y) = 50 + 220\frac{(y/r)^4}{1 + (y/r)^4}, \quad F(y) = 1.5 + \frac{5}{1 + (y/r)^4},$$

where $r = 100$. Evidently, the functions $F(y)$, $\Phi(y)$ are continuous, $F(y)$ is decreasing and $\Phi(y)$ is increasing for $y > 0$.

It worth to notice that validation of the mathematical model under consideration is outside of the scope of this paper. The interested reader is referred to the recent publications [27,28] where the topic of parameter estimation in the model of endocrine regulation with pulse-modulated feedback (i.e. (36)) is covered in depth and illustrated on actual endocrine data.

It is easily seen that the linear part of the system is FD-reducible. Obviously, the function $\det(sI_p - A_0 - A_1 \mathrm{e}^{-\tau s})$ is a polynomial with the roots $s = -b_i$, $i = 1, 2, 3$, so that the linear (continuous) part of the system is asymptotically stable for any value of τ. This is also in line with the biological nature of hormones.

Arguing in a way similar to that in [10], it can be shown that if (19) is satisfied, then there exists one and only one 1-cycle in system (36). Stability of this 1-cycle is not however guaranteed.

The effects related to the time-delay value in (36) have been investigated by numerical calculations. Fig. 1 depicts a bifurcation diagram demonstrating how the parameters of the arising periodical solutions evolve when the time-delay is varied. The system exhibits a cascade of reverse period doubling bifurcations, reducing a stable 4-cycle to a stable 1-cycle for the increasing time delay values in the range of $0 \leqslant \tau \leqslant 100$ (in minutes). Unstable solutions are not shown. Assumption (19), and thus Theorem 3, holds when $\tau < 50$ min, after that point the cycle parameters have been found by simulation of (36) until a stationary solution is reached. The assumed cumulative time delay value of $\tau = 30$ min results in a 2-cycle, a behavior that is commonly observed in the endocrine data, [28].

Apparently, an increase of the time-delay in the hybrid system (36) simplifies the dynamic pattern of the closed-loop behavior. This is an intriguing phenomenon since time delay is traditionally seen as a destabilizing factor and believed to be the main reason for sustained oscillations in endocrine [15] and other biological systems [2]. Furthermore, the results indicating less complex dynamic signaling patterns for longer times delays agree well with the fact that regular renal dialysis treatment often leads to hormone abnormalities by intervening with the hormone transport in the bloodstream. The

main endocrine derangements are sexual hormone dysfunction, thyroid abnormalities, growth retardation, hormone-related disorders of metabolism, renal osteodystrophy, and anemia, [29]. Notice that all the involved hormones are secreted in pulsatile manner and lie within the class of systems described by the model in hand.

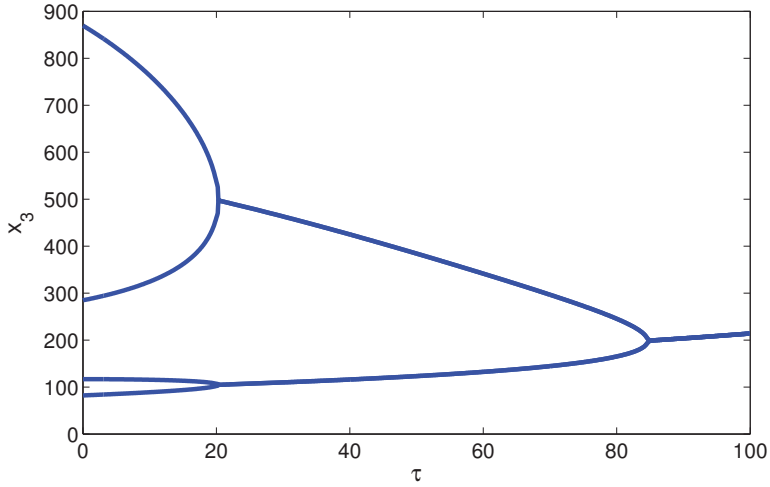

Figure 1: Bifurcation diagram. The values of x_3 (Te concentration) at the firing times t_n for different time-delays τ are depicted. Unstable solutions are not shown. A stable 4-cycle ($\tau = 0$) is reduced to a stable 1-cycle.

8 Conclusions

Dynamical phenomena in a time-delay model of non-basal (pulsatile) endocrine regulation by pulse-modulated feedback are considered. It is shown that the evolution of the resulting closed-loop hybrid system from one impulse instant to another can be described by a nonlinear discrete map. However, the system behavior in-between the impulses cannot be captured by the latter. Conditions for the existence of periodical solutions with m impulses in the least period (m-cycles) are derived and local stability conditions for the m-cycles are provided. For a specialization of the model to the case of testosterone regulation in the human male, the obtained theoretical results are confirmed by simulation and numerical calculations. It turns out that increasing time delays in the system in hand typically lead to less complex dynamic pattern of the closed-loop system solution. This somehow indicates

that the main cause of sustained oscillations in endocrine systems is not the time delay but rather the impulsive nature of the regulation mechanism.

References

[1] S.L. Lightman and B. L. Conway-Campbell, "The critical role of pulsatility activity of the HPA axis for continuous dynamic equilibration," *Nature Reviews: Neuroscience*, vol. 11, Oct., pp. 710–718, 2010.

[2] N. Radde, "The impact of time delays on the robustness of biological oscillators and the effect of bifurcations on the inverse problem," *EURASIP Journal on Bioinformatics and Systems Biology*, vol. 2009, article ID 327503, 2009.

[3] J.D. Murray, *Mathematical Biology, I: An Introduction (3rd ed.).* New York: Springer, 2002.

[4] G. Enciso and E.D. Sontag, "On the stability of a model of testosterone dynamics," *J. Math. Biol.*, vol. 49, pp. 627–634, 2004.

[5] R.H. Abraham, H. Kocak, and W.R. Smith, "Chaos and intermittency in an endocrine system model," in *Chaos, Fractals, and Dynamics*, Eds. P. Fischer and W.R. Smith, 1985, New York—Basel: Marcel Dekker, pp. 33–70.

[6] C.T. Sparrow, "Chaos in a three-dimensional single loop feedback system with a piecewise linear feedback function," *J. Math. Anal. Appl.*, vol. 83, no. 1, pp. 275–291, 1981.

[7] D. Efimov and A. Fradkov, "Oscillatority conditions for nonlinear systems with delay," *J. Appl. Math.*, article ID 72561, 2007.

[8] J.J. Walker, J.R. Terry, K. Tsaneva-Atanasova , S.P. Armstrong, C.A. McArdle, and S.L. Lightman, "Encoding and decoding mechanisms of pulsatile hormone secretion," *J. Neuroendocrinology*, vol. 22, pp. 1226–1238, 2009.

[9] A. Medvedev, A. Churilov, and A. Shepeljavyi, "Mathematical models of testosterone regulation," *Stochastic Optimization in Informatics*, (in Russian), St. Petersburg State University, vol. 2, pp. 147–158, 2006.

[10] A. Churilov, A. Medvedev, and A. Shepeljavyi, "Mathematical model of non-basal testosterone regulation in the male by pulse modulated feedback," *Automatica (IFAC journal)*, vol. 45, no. 1, pp. 78–85, 2009.

[11] Zh. Zhusubaliyev, A. Churilov, and A. Medvedev, "Bifurcation phenomena in an impulsive model of non-basal testosterone regulation," *Chaos: An Interdisciplinary Journal of Nonlinear Science*, vol. 22, no. 1, pp. 013121-1—013121-11, 2012.

[12] K. Gopalsamy and B.G. Zhang, "On delay differential equations with impulses," *J. Math. Anal. Appl.*, vol. 139, no. 1, pp. 110–122, 1989.

[13] J.O. Alzabut, "A necessary and sufficient condition for the existence of periodic solutions of linear impulsive differential equations with distributed delay," *Discrete and Continuous Dynamical Systems*, supplementary volume, pp. 35–43, 2007.

[14] W.J. Terrell, *Stability and Stabilization: An Introduction* Princeton, NJ: Princeton Univ. Press, 2009.

[15] L.S. Farhy, "Modeling of oscillations of endocrine networks with feedback," *Methods in Enzymology*, vol. 384, pp. 54–81, 2004.

[16] A. Z. Manitius and A. W. Olbrot, "Finite spectrum assignment problem for systems with delays," *IEEE Trans. Autom. Contr.*, vol. 24, no. 4, pp. 541–553, 1979.

[17] A. Medvedev, "Disturbance attenuation in finite-spectrum-assignment controllers," *Automatica (IFAC Journal)*, vol. 33, no. 6, pp. 1163–1168, 1997.

[18] A. Halanay, *Differential Equations: Stability, Oscillations, Time Lags.* New York and London: Academic Press, 1966.

[19] W.R. Smith, "Qualitative mathematical models of endocrine systems," *Am. J. Physiol*, vol. 245, no. 4, pp. R473–R477, 1983.

[20] A.Kh. Gelig and A.N. Churilov, *Stability and Oscillations of Nonlinear Pulse-modulated Systems.* Boston, MA: Birkhäuser, 1998.

[21] A. Churilov, A. Medvedev, and A. Shepeljavyi, "State observer for continuous oscillating systems under intrinsic pulse-modulated feedback," *Automatica (IFAC journal)*, vol. 48, no. 6, pp. 1005–1224, 2012.

[22] M. Cartwright and M. Husain, "A model for the control of testosterone secretion," *J. Theor. Biol.*, vol. 123, pp. 239–250, 1986.

[23] P. Das, A.B. Roy, and A. Das, "Stability and oscillations of a negative feedback delay model for the control of testosterone secretion," *BioSystems*, vol. 32, no. 1, pp. 61–69, 1994.

[24] D.M. Keenan and J.D. Veldhuis, "A biomathematical model of time-delayed feedback in the human male hypothalamic-pituitary-Leydig cell axis", *Amer. J. Physiology. Endocrinology and Metabolism*, vol. 275, no. 1, pp. E157–E176, 1998.

[25] B. Mukhopadhyay and R. Bhattacharyya, "A delayed mathematical model for testosterone secretion with feedback control mechanism," *Int. J. Mathematics and Math. Sciences*, vol. 2004, no. 3, pp. 105–115, 2004.

[26] H. Ren, "Stability analysis of a simplified model for the control of testosterone secretion," *Discrete and Continuous Dynamical Systems, Series B*, vol. 4, no. 3, pp. 729–738, 2004.

[27] E. Hidayat and A. Medvedev, "Laguerre domain identification of continuous linear time-delay systems from impulse response data," *Automatica (IFAC Journal)*, available online 15 July 2012, `http://dx.doi.org/10.1016/j.automatica.2012.06.077`.

[28] E. Hidayat and A. Medvedev, "Identification of a pulsatile endocrine model from hormone concentration data ," *IEEE Multi-Conference on Systems and Control*, October 3-5, 2012, Dubrovnik, Croatia.

[29] V. Bonomini, G. Orsoni, M. A. Sorrentino, and P. Todeschini, "Hormonal changes in hemodialysis," *Blood Purification*, vol. 4, no. 2, pp. 54–68,1990.

Paper IV

Modeling of Testosterone Regulation by Pulse-Modulated Feedback: An Experimental Data Study

Per Mattsson and Alexander Medvedev*†

September 2, 2014

Abstract

The continuous part of a hybrid (pulse-modulated) model of testosterone feedback regulation is extended with infinite-dimensional and nonlinear dynamics, to better explain the testosterone concentration profiles observed in clinical data. A linear least-squares based optimization algorithm is developed for the purpose of detecting impulses of gonadotropin-realsing hormone from measured concentration of luteinizing hormone. The parameters in the model are estimated from hormone concentration measured in human males, and simulation results from the full closed-loop system are provided.

1 Introduction

Hormones are signaling substances of endocrine systems that regulate many aspect in the human body, i.e. metabolism, growth and reproductive processes.

In the endocrine system of testosterone (Te) regulation in the male, an essential role is played by the luteinizing hormone (LH) and the gonadotropin-realising hormone (GnRH). GnRH is produced in a pulsatile (episodic) manner in the hypothalamus and stimulates the secretion of LH into the blood by the pituitary gland. LH stimulates in turn the secretion of Te by the

*This research has been supported by the European Research Council (ERC) via the Advanced Grant 247035.

†P. Mattsson and A. Medvedev are with the department of Information Technology, Uppsala University, Uppsala, Sweden.

testes. The endocrine feedback is then closed by Te inhibiting the secretion of both GnRH and LH [1].

Understanding testosterone regulation is important in, for example, the treatment of prostate cancer and reproductive failure. Changes in the GnRH secretion pattern are also implicated in aging and obesity [1].

In the literature, numerous mathematical models of Te regulation have been suggested, mostly without taking into account the episodic secretion of GnRH. In [2], a parsimonious pulse-modulated model of the GnRH-LH-Te axis was presented. This model was extended in [3] to cover the time delay phenomena corresponding to the LH secretion in the pituitary gland and transportation of the hormone to the testes. The resulting hybrid and time-delayed model still lends itself to mathematical analysis, and much is already known about its behaviors [4]. It generally exhibits periodical solutions of a wide periodicity range as well as deterministic chaos. The concentration profiles of GnRH and LH produced by the model are consistent with experimental data. For instance, this model was successfully used in [5] to estimate GnRH impulses, given measured concentrations of LH. Yet, it seems to be hard to select the model parameters in such a way that the simulated Te concentration evolves similarly to the measurements. One reason for this is that, in the current model, the secretion of Te never saturates.

A data-driven and biologically motivated mathematical model for Te regulation has also been studied in e.g. [6]. Here the saturation of secretion rates is an integral part and the hormone trends fit the measurements well. However, the model is not equipped with a pulse-modulated feedback mechanism and its closed-loop dynamics have not been studied analytically.

When a model structure is decided, the parameters of the model must be determined from measured data. For this, techniques from statistics and system identification can be used. In the human, the GnRH concentration is typically not measured due to ethical reasons. Therefore the GnRH impulses have to be estimated from measured LH and Te concentrations instead.

In the present paper, the model analyzed in [3] is extended in view of the results in [6]. Furthermore, a new method for estimating GnRH impulses from clinical LH data is briefly presented. Some initial results on identifying the LH feedforward action on the secretion of Te are also given. Finally, closed-loop simulation results for the model are provided.

2 Background

The underlying dynamics of Te regulation in the male can be described by the Smith model, c.f. [7], that is given by the following ordinary differential

equations

$$\begin{aligned}\dot{R} &= f(T) - B_1(R),\\ \dot{L} &= G_1(R) - B_2(L),\\ \dot{T} &= G_2(L) - B_3(T),\end{aligned}$$

where $R(t)$, $L(t)$ and $T(t)$ represent the serum concentration of GnRH, LH and Te respectively. The non-negative functions B_1, B_2, B_3 describe clearing rates of the hormones and G_1, G_2, f specify the rates of their secretion.

The model in [3] is a generalization of the above Smith model, where the feedback function $f(T)$ is replaced by a pulse modulation operator, to capture the well-known pulsatile nature of GnRH secretion. The functions B_1, B_2, B_3, G_1 and G_2 were approximated by linear functions to facilitate the analysis.

In [6] another model, where the functions G_1 and G_2 are nonlinear saturating functions, is presented. This saturation is biologically motivated, and clinical data indicate that the saturation in G_2 plays an important role.

In the next section a new model that combines the pulse-modulated feedback in [3] with saturating secretion is proposed.

3 Mathematical Model

Consider now a system in vector-matrix form with the continuous state vector $x \in \mathbb{R}^3$, where $x_1 = R(t)$, $x_2 = L(t)$ and $x_3 = T(t)$. The model considered in this contribution can then be expressed as

$$\dot{x}(t) = A_0 x(t) + A_1 \Phi_L(t-\tau) + \beta, \qquad y(t) = Cx(t), \tag{1}$$

$$t_{k+1} = t_k + T_k, \qquad x(t_k^+) = x(t_k^-) + \lambda_k B, \tag{2}$$

$$T_n = \Phi(y(t_k)), \qquad \lambda_k = F(y(t_k)), \tag{3}$$

where

$$A_0 = \begin{bmatrix} -b_1 & 0 & 0 \\ g_1 & -b_2 & 0 \\ 0 & 0 & -b_3 \end{bmatrix}, \quad A_1 = \begin{bmatrix} 0 & 0 & 0 \\ 0 & 0 & 0 \\ 0 & g_2 & 0 \end{bmatrix},$$

$$B = \begin{bmatrix} 1 \\ 0 \\ 0 \end{bmatrix}, \text{ and } C = \begin{bmatrix} 0 & 0 & 1 \end{bmatrix},$$

and $\beta \in \mathbb{R}^3$ describes the basal secretion of the hormones. Therefore, the basal secretion is seen as a constant signal exogenous to the endocrine regulation loop. According to (2), the continuous state vector x undergoes jumps at the time instances t_k, and the amplitudes of these jumps are determined

by the impulse weights λ_k. The frequency and amplitude modulation functions $\Phi(\cdot)$, and $F(\cdot)$ are assumed to be Hill functions of the form

$$\Phi(y) = k_1 + k_2\frac{(y/h)^p}{1+(y/h)^p}, \quad F(y) = k_3 + \frac{k_4}{1+(y/h)^p},$$

where $p \in \mathbb{N}^+$ is the (positive integer) order of the Hill function and $k_1, k_2, k_3, k_4, h \in \mathbb{R}^+$. Notice that both modulation functions are monotone and bounded. Furthermore, $\Phi_L(t)$ captures the feedforward action of LH on Te. Following the reasoning in e.g. [6], this signal is exerted via a time average of the momentaneous LH concentration. Also, since there is an upper limit to the amount of Te that can be secreted during any given time-interval, this signal should pass through a saturation function. For the purpose of this paper, the saturation function has been chosen to be a Hill function, more specifically

$$\Phi_L(t) = \frac{(H_L(t)/h_L)^{p_L}}{1+(H_L(t)/h_L)^{p_L}}, \quad H_L(t) = \frac{1}{\ell}\int_{t-\ell}^{t} L(s)ds, \tag{4}$$

where ℓ is the length of the sliding window. Finally, τ corresponds to the time it takes for LH to travel from pituitary to the testes. The measurable hormone concentrations are those of Te and LH.

Comparing the model here with the one in [3], it can be seen that the only difference between them is that the equation

$$\dot{x}(t) = A_0x(t) + A_1x(t-\tau)$$

in [3] has been replaced with (1).

4 Estimating the GnRH Impulses

To consider how GnRH impulses affect LH concentration, it is sufficient to study the first two states of x, so let $\tilde{x} = \begin{bmatrix} x_1(t) & x_2(t) \end{bmatrix}^T$. Then it follows from (1) - (3) that

$$\dot{\tilde{x}} = \tilde{A}\tilde{x} + \tilde{B}\xi(t) + \tilde{\beta}, \tag{5}$$

$$x_2(t) = \tilde{C}\tilde{x}(t), \tag{6}$$

where

$$\tilde{A} = \begin{bmatrix} -b_1 & 0 \\ g_1 & -b_2 \end{bmatrix}, \quad \tilde{B} = \begin{bmatrix} 1 \\ 0 \end{bmatrix}, \quad \tilde{\beta} = \begin{bmatrix} \beta_1 \\ \beta_2 \end{bmatrix}, \quad \tilde{C} = \begin{bmatrix} 0 & 1 \end{bmatrix},$$

and

$$\xi(t) = \sum_{k=0}^{\infty} \lambda_n \delta(t - t_k). \tag{7}$$

The expression in (7) is simply an alternative way of describing the jumps in (2) as a weighted train of Dirac delta-functions $\delta(\cdot)$. If (5) is subject to the initial condition $\tilde{x}(t_o) = \tilde{x}_o = \begin{bmatrix} x_{o,1} & x_{o,2} \end{bmatrix}^T$, then

$$x_2(t) = \tilde{C}\left(e^{\tilde{A}(t-t_o)}\tilde{x}_o + \int_{t_o}^{t} e^{\tilde{A}(t-s)}(\tilde{\beta} + \tilde{B}\xi(s))ds \right).$$

By evaluating the integral, this can be rewritten as

$$x_2(t) = \tilde{C}e^{\tilde{A}(t-t_o)}\tilde{x}_o + \tilde{C}\tilde{A}^{-1}\left(e^{\tilde{A}(t-t_o)} - I\right)\tilde{\beta} + \sum_{k=0}^{\infty} g_1\lambda_k z(t-t_k), \qquad (8)$$

where

$$z(t) = \frac{e^{-b_2 t} - e^{-b_1 t}}{b_1 - b_2}H(t),$$

and $H(\cdot)$ is the Heaviside step function. From (8), it can be seen that the unknown parameter g_1 always appear in product with other unknown parameters, e.g. the impulse weights λ_k. It is therefore not possible to uniquely determine g_1 from measured data. Similarly, it is in practice not possible to separate β_1 from β_2 when the data are collected from the closed loop system. Since the GnRH concentration is not measurable in the human for ethical reasons, it is assumed that $g_1 = 1$ and $\beta_1 = 0$. Thus, any estimated GnRH signal should be considered as a virtual signal, providing information about the GnRH firing times t_k and the ratios between the weights λ_k. However, the actual concentration might differ in the real system. Also notice that $g_1 = 1$ and $\beta_1 = 0$ imply

$$\tilde{C}e^{\tilde{A}(t-t_o)}\tilde{x}_o = x_{o,1}z(t-t_o) + x_{o,2}e^{-b_2(t-t_o)},$$
$$\tilde{C}\tilde{A}^{-1}\left(e^{\tilde{A}(t-t_o)} - I\right)\tilde{\beta} = \left(1 - e^{-b_2(t-t_o)}\right)\frac{\beta_2}{b_2}.$$

A method for identifying the parameters and firing times in (5) was proposed in [8]. However, the method, in its present form, is restricted to the identification of two impulses at a time. A general method for estimating unknown input impulses was also developed in [9], but it assumes continuous access to the output data, and is therefore hard to apply directly on LH data where the data sampling is typically slow (e.g. 10 min). To be able to handle longer and under-sampled data sets, a new method is proposed in the next section.

4.1 Estimating firing times and weights

First let $b_1 > b_2$, an assumption that is biologically reasonable in the GnRH-LH-Te axis, see e.g. [6]. The data are assumed to be collected at the times

$\hat{t}_0, \hat{t}_1, \ldots, \hat{t}_m$, where $\hat{t}_0 = 0$. Also assume that $t_1, \ldots, t_n$ are all firing times in the interval $(0, \hat{t}_m)$. Let

$$\begin{aligned}
z_i &= \left[(1 - e^{-b_2 \hat{t}_i})/b_2 \quad e^{-b_2 \hat{t}_i} \quad z(\hat{t}_i) \quad z(\hat{t}_i - t_1) \quad \cdots \quad z(\hat{t}_i - t_n)\right], \\
Z &= \begin{bmatrix} z_1^T & \cdots & z_m^T \end{bmatrix}^T, \\
G &= \begin{bmatrix} \beta_2 & x_{o,2} & x_{o,1} & \lambda_1 & \cdots & \lambda_n \end{bmatrix}^T, \\
Y &= \begin{bmatrix} x_2(\hat{t}_0) & \cdots & x_2(\hat{t}_m) \end{bmatrix}.
\end{aligned}$$

Then it can be seen from (8) that

$$ZG = Y.$$

So, if the firing times t_k and system parameters are known, then the impulse weights, initial conditions and basal secretion can be found by solving the following nonnegative linear least-squares problem:

$$\begin{aligned}
&\min_{G} \quad \|ZG - Y\|_2^2, \\
&\text{s.t.} \quad G \geq 0,
\end{aligned} \tag{9}$$

where the inequality in the constraint is understood element-wise and follows from the biology of the system.

When the firing times are not known, the values of t_k in Z can be "guessed" by gridding. The following algorithm provides a way of choosing the grid points.

Algorithm 1. *Solve* (9) *with all grid points at the sampling times. If two consecutive grid points $\hat{t}_l$ and $\hat{t}_{l+1}$ have been assigned the non-zero weights $\hat{\lambda}_l$ and $\hat{\lambda}_{l+1}$, replace those impulses with one impulse fired at the time*

$$t_k = \hat{t}_l + \frac{1}{b_2 - b_1} \ln\left(1 + \frac{\hat{\lambda}_{l+1}\left(e^{b_2 \Delta} - e^{b_1 \Delta}\right)}{\hat{\lambda}_l + \hat{\lambda}_{l+1} e^{b_1 \Delta}}\right)$$

and with the impulse weight

$$\lambda_k = e^{-b_1 (t_k - \hat{t}_l)} \left(\hat{\lambda}_{l+1} e^{b_1 \Delta} + \hat{\lambda}_l\right),$$

where $\Delta = \hat{t}_{l+1} - \hat{t}_l$.

Proposition 1. *Assume that the data in Y are generated according to* (8)*, that $b_1 > b_2 > 0$, and that there are at least three sampling instances in between any two firing times. Then Algorithm 1 yields the true firing times and impulse weights.*

Proof. Omitted due to the page limitation. □

It should be noticed that the assumption about three sampling times in between any two firing times is only needed to guarantee uniqueness of the solution. Algorithm 1 produces a solution even if the firing times are closer to each other.

In real data, however, the measurements in Y will be corrupted by disturbances. In that case, following Algorithm 1 will typically result in solutions where every grid point is assigned a non-zero impulse weight. A common way to work around this problem and find sparser solutions is to put a constraint on the sum of the (positive) impulse weights, i.e. the l_1-norm, see e.g. [10]. This leads to the following optimization problem,

$$\begin{aligned} \min_{G} \quad & \|ZG - Y\|_2^2, \\ \text{s.t} \quad & \sum \lambda_k < \lambda_{\max} \\ & G \geq 0 \end{aligned} \tag{10}$$

that can be solved efficiently by existing methods, see e.g. [11]. In the case studied here, i.e. estimating GnRH impulses from LH data, it is usually possible to find a value of $\lambda_{\max}$ that gives sparse solutions with good fit, as seen in the forthcoming sections.

4.2 Estimating the parameters

To set up the optimization problem in (10), the parameters b_1 and b_2 are needed. According to biological data provided in [6],

$$\begin{aligned} 0.23 \text{ min}^{-1} \leq b_1 \leq 0.69 \text{ min}^{-1}, \\ 0.0087 \text{ min}^{-1} \leq b_2 \leq 0.014 \text{ min}^{-1}. \end{aligned}$$

In this contribution, the parameters have been chosen by gridding over these intervals, solving the optimization problem for all possible combinations, and finally picking the solution that gives the best fit.

5 Estimating the Testosterone Dynamics

In this section some preliminary results on the identification of the Te part of the model are presented. Recall that it follows from (1)-(3) that

$$\dot{T}(t) = \dot{x}_3(t) = -b_3 x_3(t) + g_2 \Phi_L(t - \tau) + \beta_3. \tag{11}$$

Assuming the function $\Phi_L(\cdot)$ and the delay τ to be known, standard methods for linear system identification can be used to identify the parameters b_3,

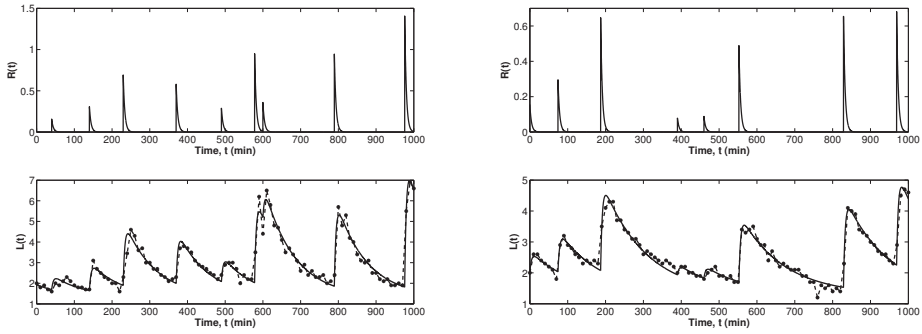

Figure 1: Result of GnRH impulses estimation. Upper row shows the estimated virtual GnRH levels for each patient. Bottom row shows the estimated LH levels (solid line) together with the measured data (dashed line with dots at each sampling time). The data in the left column are from a patient that is 27 years old, and in the right column from a 40 years old patient.

g_2 and β_3. Here the ordinary least-squares method is used to solve the regression problem, see e.g. [12]. However, the parameters values for h_L, p_L and ℓ are still needed in (4). At this stage, the parameters are simply chosen by gridding over reasonable intervals. In the future, it is planned to look more into the model structure in (11) and possible identification methods.

6 Experimental Results

The methods developed in this paper have been tested on LH and Te concentrations measured in 18 healthy human males. The data was collected for 17 hours and sampled every 10 minutes, see [13] for a description of the data and experimental protocol.

For all patients, the LH data were well explained by the model in (5), with a sparse set of impulses (4-10 impulses in 1000 minutes). For illustration, the results of two patients are shown in Fig. 6.

To test the identification of the testosterone dynamics, (11) was simulated with the measured LH as input. It should be noted that such a simulation cannot be considered a complete estimation of the testosterone concentration since it only shows the Te secreted due to the LH feedforward signal and the constant basal secretion. In the actual endocrine system, the concentration of Te is also involved in other regulations and events outside the GnRH-LH-Te loop, both of endocrine and non-endocrine nature [14]. However, the simulation results with measured LH data indicate that the

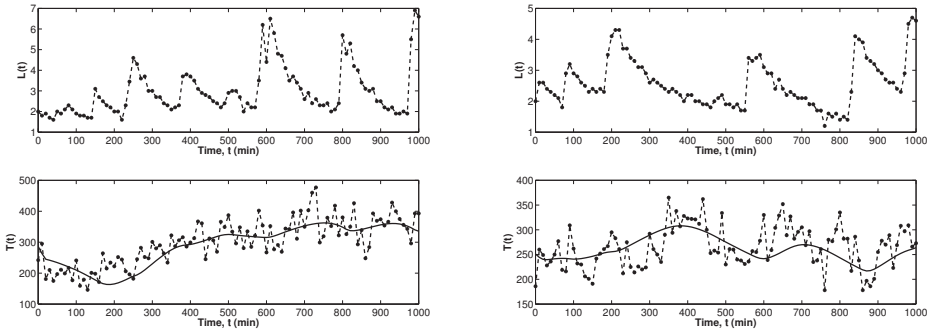

Figure 2: Result of Te dynamics identification. The upper row shows the measured LH data that are used as input. The bottom row shows measured Te (dashed line) together with Te concentration given by simulation of the model (solid line). The left column corresponds to data from a 27 years old patient, and the right column from a 40 years old patient.

simulated Te concentration still follows the general trend in the corresponding measured Te data. For illustration, the results for the same two patients as above are shown in Fig. 6. Yet, the identification of Te still needs to be investigated in more detail, both when it comes to the model structure and the suitable identification methods.

7 Simulations of the Closed-Loop System

In this section, the complete model described by (1)-(3) is simulated. The model parameters are identified from of the LH and Te data collected from a 27 years old and a 40 years old healthy individuals. The modulation functions in (3) were then chosen so that the minimum and maximum time between impulses corresponded to the minimum and maximum inter-impulse times in the real data.

To imitate the clinical conditions, the simulated data were sampled every 10 minutes with white Gaussian measurement noise added. Fig. 7 and Fig. 7 compare the results of the closed-loop simulation with the experimental data that the parameters have been estimated from. Since the modulation functions in the feedback are not formally identified from measurements, it can not be expected that the simulated data and the real data should look exactly the same. However, it can be seen that the simulated and real data in many ways behave similarly. For example, the numbers of impulses are about the same, the hormone concentration are of the same level, etc.

One important difference is that the amplitude of the LH pulses seem to

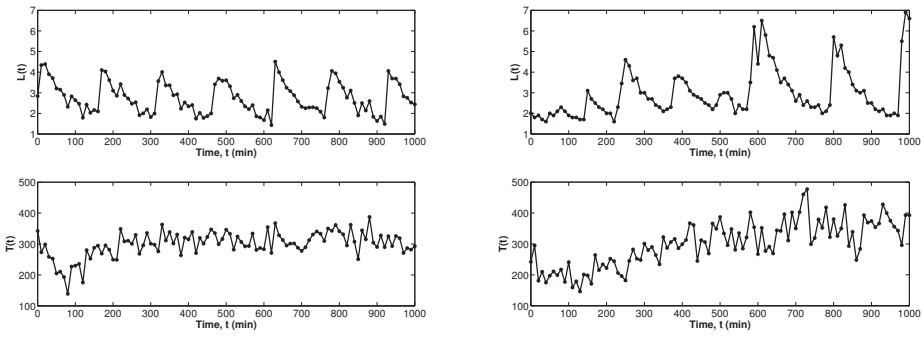

Figure 3: Simulation of the closed-loop system. Left column: simulation; right column: measured data in a 27 years old patient.

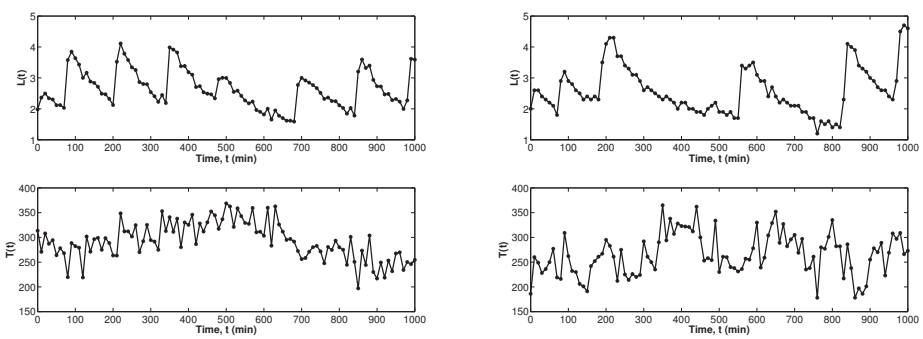

Figure 4: Simulation of the closed-loop system. Left column: simulation; right column: measured data in a 40 years old patient.

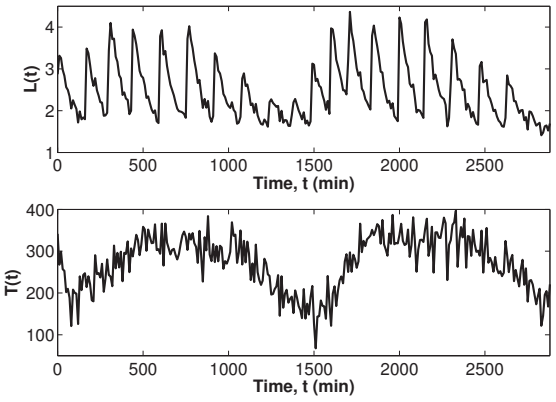

Figure 5: Simulation over 48 hours, with circadian rhythm.

vary more over time in the real data. It has been seen in previous studies that there is a prominent circadian rhythm in Te concentrations [15]. This phenomenon can be incorporated by several means in the model developed in this paper. For example, the amplitude modulation function could depend on time in a periodic manner. However, to study such periodic behaviour it would be desirable to have data sets that span over at least two full days. Fig. 7 presents a simple example with the same parameters as in Fig. 7, except that the amplitude modulation function is multiplied by a sinusoid function with a period of 24 hours.

8 Conclusions and Future Work

A new hybrid mathematical model of endocrine regulation in the GnRH-LH-Te axis is suggested, together with an algorithm for estimating the firing times of GnRH impulses from time series of measured LH concentrations.

Tests on hormone data collected in healthy human males indicate that the model explains the experimental LH concentration profile very well with a sparse set of GnRH impulses. An initial study on system identification of the testosterone dynamics is also presented. The results show that the model captures the changes in the Te secretion due to changes of LH concentration. However, further research into the Te secretion model structure, along with more refined identification methods, is still needed.

With the parameter estimates obtained by identification from experimental data, the simulated complete closed-loop system exhibits behaviors similar to the clinical data. Further work on estimation of the modulation functions in the feedback from Te to GnRH is needed. Also, the circadian

rhythm should be incorporated into the modulation functions to enhance model fidelity. To achieve these goals, more clinical data have to be collected.

References

[1] J. D. Veldhuis, "Recent insights into neuroendocrine mechanisms of aging of the human male hypothalamic-pituitary-gonadal axis," *Journal of Andrology*, vol. 20, no. 1, pp. 1–18, 1999.

[2] A. Churilov, A. Medvedev, and A. Shepeljavyi, "Mathematical model of non-basal testosterone regulation in the male by pulse modulated feedback," *Automatica*, vol. 45, no. 1, pp. 78–85, 2009.

[3] A. Churilov, A. Medvedev, and P. Mattsson, "Analysis of a pulse-modulated model of endocrine regulation with time-delay," in *IEEE 51st Annual Conference on Decision and Control (CDC), 2012*, 2012, pp. 362–367.

[4] ——, "Finite-dimensional reducibility of time-delay systems under pulse-modulated feedback," in *IEEE 52st Annual Conference on Decision and Control (CDC), 2013*, 2013.

[5] E. Hidayat and A. Medvedev, "Identification of a pulsatile endocrine model from hormone concentration data," in *Control Applications (CCA), 2012 IEEE International Conference on*, 2012, pp. 356–363.

[6] D. M. Keenan and J. D. Veldhuis, "A biomathematical model of time-delayed feedback in the human male hypothalamic-pituitary-leydig cell axis," *American Journal of Physiology-Endocrinology And Metabolism*, vol. 275, no. 1, pp. E157–E176, 1998.

[7] W. R. Smith, "Qualitative mathematical models of endocrine systems," *American Journal of Physiology-Regulatory, Integrative and Comparative Physiology*, vol. 245, no. 4, pp. R473–R477, 1983.

[8] E. Hidayat and A. Medvedev, "Laguerre domain identification of continuous linear time-delay systems from impulse response data," *Automatica*, vol. 48, no. 11, pp. 2902 – 2907, 2012.

[9] P. Mattsson and A. Medvedev, "Estimation of input impulses by means of continuous finite memory observers," in *American Control Conference*, june 2012, pp. 6769–6774.

[10] R. Tibshirani, "Regression shrinkage and selection via the lasso," *Journal of the Royal Statistical Society. Series B (Methodological)*, vol. 58, no. 1, pp. pp. 267–288, 1996.

[11] S. Boyd and L. Vandenberghe, *Convex Optimization*. New York, NY, USA: Cambridge University Press, 2004.

[12] T. Söderström and P. Stoica, *System identification*. Upper Saddle River, NJ, USA: Prentice-Hall, Inc., 1988.

[13] D. M. Keenan, I. J. Clarke, and J. D. Veldhuis, "Noninvasive analytical estimation of endogenous gnrh drive: Analysis using graded competitive gnrh-receptor antagonism and a calibrating pulse of exogenous gnrh," *Endocrinology*, vol. 152, no. 12, pp. 4882–4893, 2011.

[14] M. Zitzmann and E. Nieschlag, "Testosterone levels in healthy men and the relation to behavioural and physical characteristics: facts and constructs," *European Journal of Endocrinology*, vol. 144, no. 3, pp. 183–197, 2001.

[15] J. D. Veldhuis, J. C. King, R. J. Urban, A. D. Rogol, W. S. Evans, L. A. Kolp, and M. L. Johnson, "Operating characteristics of the male hypothalamo-pituitary-gonadal axis: pulsatile release of testosterone and follicle-stimulating hormone and their temporal coupling with luteinizing hormone," *J Clin Endocrinol Metab*, vol. 65, no. 5, pp. 929–41, 1987.

Recent licentiate theses from the Department of Information Technology

2014-005 Thomas Lind: *Change and Resistance to Change in Health Care Inertia in Sociotechnical Systems*

2014-004 Anne-Kathrin Peters: *The Role of Students' Identity Development in Higher Education in Computing*

2014-003 Liang Dai: *On Several Sparsity Related Problems and the Randomized Kaczmarz Algorithm*

2014-002 Johannes Nygren: *Output Feedback Control - Some Methods and Applications*

2014-001 Daniel Jansson: *Mathematical Modeling of the Human Smooth Pursuit System*

2013-007 Hjalmar Wennerström: *Meteorological Impact and Transmission Errors in Outdoor Wireless Sensor Networks*

2013-006 Kristoffer Virta: *Difference Methods with Boundary and Interface Treatment for Wave Equations*

2013-005 Emil Kieri: *Numerical Quantum Dynamics*

2013-004 Johannes Åman Pohjola: *Bells and Whistles: Advanced Language Features in Psi-Calculi*

2013-003 Daniel Elfverson: *On Discontinuous Galerkin Multiscale Methods*

2013-002 Marcus Holm: *Scientific Computing on Hybrid Architectures*

2013-001 Olov Rosén: *Parallelization of Stochastic Estimation Algorithms on Multicore Computational Platforms*

UPPSALA
UNIVERSITET

Department of Information Technology, Uppsala University, Sweden